



Universiteit  
Leiden  
The Netherlands

## Ecological functions and environmental fate of exopolymers of *Acidobacteria*

Costa, O.Y.A.

### Citation

Costa, O. Y. A. (2020, July 9). *Ecological functions and environmental fate of exopolymers of Acidobacteria*. Retrieved from <https://hdl.handle.net/1887/123274>

Version: Publisher's Version

License: [Licence agreement concerning inclusion of doctoral thesis in the Institutional Repository of the University of Leiden](#)

Downloaded from: <https://hdl.handle.net/1887/123274>

**Note:** To cite this publication please use the final published version (if applicable).

Cover Page



Universiteit Leiden



The handle <http://hdl.handle.net/1887/123274> holds various files of this Leiden University dissertation.

**Author:** Costa, O.Y.A.

**Title:** Ecological functions and environmental fate of exopolymers of Acidobacteria

**Issue Date:** 2020-07-09

---

# Chapter 3

*Transcriptional and proteomic responses of Granulicella sp. WH15 to increasing concentrations of cellobiose*

---

Ohana Y.A. Costa<sup>#</sup>, Marcelo M. Zerillo<sup>#</sup>, Daniela Zühlke, Anna M. Kielak, Agata Pijl, Katharina Riedel, Eiko E. Kuramae

<sup>#</sup> equal contribution

Modified version published as: Costa OYA, Zerillo M, Zühlke D, Kielak AM, Pijl A, Riedel K, Kuramae EE (2020). Responses of *Acidobacteria Granulicella* sp. WH15 to High Carbon Revealed by Integrated Omics Analyses. **Microorganisms**. 8(2).

## Abstract

The phylum *Acidobacteria* is widely distributed in soils, but few representatives have been cultured. In general, *Acidobacteria* are oligotrophs and exhibit slow growth under laboratory conditions. We sequenced the genome of *Granulicella* sp. WH15, a strain obtained from decaying wood, and determined the transcriptome and proteome when grown in poor medium with a low or high concentration of cellobiose. We detected the presence of 217 carbohydrate-associated enzymes in the genome of strain WH15. Integrated analysis of the transcriptomic and proteomic profiles suggested that high concentration of cellobiose triggered the expression of stress-related proteins. As part of this response, transcripts related to cell wall stress, such as sigma factor  $\sigma^W$  and toxin-antitoxin (TA) systems, were upregulated, as were several proteins involved in detoxification and repair, including the multidrug resistance protein MdtA and outer membrane protein OprM. KEGG metabolic pathway analysis indicated repression of carbon metabolism upon high cellobiose concentration, especially the pentose phosphate pathway, and repression of protein synthesis, carbohydrate metabolism and cell division, suggesting arrest of cell activity and growth. In summary, the stress response of *Granulicella* sp. WH15 induced by the presence of a high cellobiose concentration in the medium resulted in the enhanced expression of functions associated with secretion of metabolic byproducts and with reallocation of resources to cell maintenance instead of growth.

**Keywords:** Genome, Transcriptome, Proteome, Oligotroph, stress signal, transporters, sigma factor  $\sigma^W$

## 1. Introduction

*Acidobacteria* is one of the most abundant bacterial phyla in soil, yet little is known about its physiology, ecological function, and impact on the soil environment (Kielak *et al.*, 2016). The first species of *Acidobacteria* was described in the 1990s (Kishimoto *et al.*, 1991), and the ubiquity of the phylum was only recognized after the introduction of 16S rRNA gene sequencing and metagenomics (Kielak *et al.*, 2016). This phylum constitutes 20–50% of the soil bacterial community (Kuramae *et al.*, 2012, Navarrete *et al.*, 2013, Pan *et al.*, 2014, Kielak *et al.*, 2016, Kielak *et al.*, 2016), but the few species that have been isolated exhibit slow growth under standard laboratory conditions, resulting in a relatively small number of cultured representatives. Genome analyses have revealed only one or two copies of the 16S rRNA gene in species sequenced to date (Wingender *et al.*, 1999, Pankratov & Dedysch, 2010, Whang *et al.*, 2014), which may indicate slow growth of these bacteria under natural conditions as well. Ribosomal RNA operon copy number has been potentially linked to low environmental resource availability and slow growth rate in bacteria (Valdivia-Anistro *et al.*, 2016). Consequently, the factor(s) responsible for the prevalence and successful adaptation of *Acidobacteria* to soil conditions remain unclear.

A strong negative correlation between *Acidobacteria* abundance based on 16S rRNA amplicon next generation sequences and soil organic carbon content has been observed in diverse microbiome studies, suggesting that the phylum is composed of oligotrophic bacteria (Fierer *et al.*, 2007, Foessel *et al.*, 2014). Oligotrophs are mainly characterized by their capacity to grow under low nutrient availability and their higher substrate utilization efficiency than copiotrophs, producing a higher biomass yield per unit of substrate utilized. In general, they are able to thrive in poor nutrient environments and exhibit slow growth under laboratory conditions (Ho *et al.*, 2017). Although most acidobacterial isolates have been obtained from low-nutrient culture media, some isolates are capable of growing at higher sugar concentrations (de Castro *et al.*, 2013, Campanharo *et al.*, 2016, Kielak *et al.*, 2016).

Many soil *Acidobacteria* are able to degrade a wide range of carbon sources, mainly mono- and disaccharides, such as glucose, xylose, mannose, galactose and cellobiose. Predictions of genes associated with the degradation of polysaccharides in acidobacterial genomes have not always been confirmed by experimental data (Kielak *et al.*, 2016). This knowledge gap highlights the need for studies with cultured strains. We recently established a culture medium and incubation conditions permitting larger amounts of acidobacterial biomass (cells and/or exopolysaccharides, EPS) to be harvested after 4 days of incubation (Campanharo *et al.*, 2016); by contrast, on other reported media, most cultivated acidobacterial species form visible colonies only after weeks of incubation (Ward *et al.*, 2009). As no study has addressed the response of acidobacterial strains under different cellobiose concentrations, the aim of this study was to sequence the genome of an acidobacterial strain, *Granulicella* sp. WH15, and determine the transcriptome and proteome responses under conditions of low (0.025%) and high (3%) cellobiose concentrations.

## 2. Material and Methods

### 2.1. Genome

The *Granulicella* sp. WH15 strain (Valášková *et al.*, 2009) obtained from the collection of the Netherlands Institute of Ecology (NIOO-KNAW) was grown on 1/10 TSB agar medium (Valášková *et al.*, 2009) at pH 5.0 for 3 days at 30 °C. The bacterial cells were harvested and the genomic DNA was extracted using MasterPure™ DNA Purification Kit (Epicentre, Madison, WI) according to manufacturer's instructions. A total of 10 mg of DNA was sent to the Genomics Resource Center (Baltimore, USA) for a single long insert library (15kb-20kb), that was constructed and sequenced in one SMRTcell using the PacBio RS II (Pacific Biosciences, Inc.) sequencing platform. *De novo* assembly was performed with the help of SMRT Analysis software v2.2.0 (Pacific Biosciences) featuring HGAP 2 (Chin *et al.*, 2013), and subsequent correction with Pilon 1.16 (Walker *et al.*, 2014) to reveal a circular replicon: a 4,675,153-bp chromosome (G+C content 60,7%; 58.4× coverage). Automatic gene prediction and annotation was performed by using Prokka (Seemann, 2014), RAST genome annotation server (<http://rast.nmpdr.org/>) (Aziz *et al.*, 2008). Genes were mapped to COG and KEGG IDs using the COG database (2014 release) (Galperin *et al.*, 2015) and KEGG database (release 2013) (Kanehisa, 2000), using in house scripts. The CAZyme contents of WH15 genome were determined by identifying genes containing CAZyme domains using the dbCAN2 meta server ([cys.bios.niu.edu/dbCAN2](http://cys.bios.niu.edu/dbCAN2)) (Zhang *et al.*, 2018), according to the CAZy (Carbohydrate-Active Enzyme) database classification (Lombard *et al.*, 2014). Only CAZyme domains predicted by at least two of the three algorithms (DIAMOND, HMMER and Hotpep) employed by dbCAN2 were kept. Circular genome map was drawn used CGView software (Stothard & Wishart, 2004). The *Granulicella* sp. WH15 strain genome data is deposited at NCBI with accession number CP042596.

### 2.2. Growth experiments

CAZyme annotation was compared to *in vitro* carbohydrate utilization assays. Modified 1/10 TSB (1.7 g of casein hydrated (acid) (Oxoid™), 0.3 g of tryptone (vegetable) (Fluka 95039), 0.5 g of sodium chloride, 0.25 g of dipotassium phosphate (Sigma-Aldrich) in 1 liter of distilled water) pH 5.0 medium was supplemented with sole carbon sources: pectin (apple – Sigma- Aldrich), glycogen (Sigma- Aldrich), glucosamine (Sigma- Aldrich) and cellulose (Sigma- Aldrich), at 1% (w/v), and D-glucose, D-galactose, D-mannose, D-xylose, L- arabinose, L-rhamnose, D-galacturonic acid, cellobiose, D-lactose, and sucrose at 25 mM. Plates were inoculated with 100 µL of cell suspension at  $OD_{600nm} = 1$  obtained from modified TSB (3% of cellobiose), homogenized and incubated at 30 °C for 72 h, when growth was evaluated. After 72 h of growth, colonies were reinoculated in a new plate with the same carbohydrate concentration, and the process was repeated three times, in order to confirm growth.

### 2.3. Transcriptome

Bacteria were grown in two sugar concentrations, based on solid (1.5% agarose) modified 1/10 TSB medium pH 5.0 (as described above) supplemented with 0.025% and 3% of cellobiose, for low and high cellobiose conditions, respectively. Plates were inoculated with 100  $\mu$ L of cells at  $OD_{600nm} = 1$  nm/mL, homogenized and incubated at 30 °C for 72 h. RNA extraction was performed using Aurum Total RNA kit (Bio-Rad) in a final volume of 50  $\mu$ L of elution buffer. Total of 6 mg of RNA was rRNA depleted with the Ribo-Zero Bacteria Kit from Illumina. The sequencing library of each sample was prepared with the Kapa Biosystems Stranded RNA-Seq kit, and sequenced according to the Illumina TruSeq v3 protocol on the HiSeq2000 with a single read 50 bp and 7bp index at Erasmus Center for Biomics (Rotterdam). Quality of the raw fastq files was checked and filtered with FastQC. Read alignment was performed on the genome of WH15 using Bowtie2 (Langmead & Salzberg, 2012). Differential expression profiling was performed between low and high cellobiose treatments. Gene expression levels were quantified using software package RNASeq by Expectation Maximization (RSEM) (Li & Dewey, 2011). The matrix of fragment counts from each sample was used for the differential expression analysis via edgeR package. All samples were normalized by trimmed mean of M-values (TMM). (Robinson *et al.*, 2009). Differentially expressed genes between the two treatments, using low cellobiose treatment as a reference, were identified at significance level of 0.05 with a false discovery rate (FDR) correction method and the  $\log_2$  fold change (logFC) equaled to 1. 1% differentially expressed genes were selected to generate a heatmap. COG (Galperin *et al.*, 2015) and KEGG (Kanehisa, 2000) analysis were performed for differentially expressed genes. Transcriptome data is deposited at NCBI GEO database with accession number GSM4017160-65.

### 2.4. Analysis of the cytosolic proteome by mass spectrometry and data analysis

Bacteria were grown in the same low cellobiose (0.025% cellobiose) and high cellobiose (3% of cellobiose) conditions for transcriptome analyses. Bacterial biomass from each low and high cellobiose treatment were collected from plates and resuspended in 1 ml TE buffer. Bacterial cells were harvested by centrifugation 10,015 x g at 4 °C for 10 min. Pellets were washed twice with 1 mL of TE buffer and finally resuspended in 1 ml TE buffer. 500 $\mu$ L of cell suspension were transferred into 2 mL screw cap tubes filled with 500  $\mu$ L glass beads (0.1 mm in diameter; Sarstedt, Germany) and mechanically disrupted using Fastprep (MP Biomedicals) for 3 x 30 sec at 6.5 m/s; with on ice incubation for 5 min between cycles. To remove cell debris and glass beads samples were centrifuged for 10 min at 4 °C at 21,885 x g, followed by a second centrifugation (30 min at 4 °C at 21,885 x g) to remove insoluble and aggregated proteins. The protein extracts were kept at -20 °C. Protein concentration was determined using RotiNanoquant (Carl Roth, Germany). Proteins were separated by SDS-PAGE. Protein lanes were cut into ten equidistant pieces and in-gel digested using trypsin as described earlier (Grube *et al.*, 2014). Tryptic peptides were separated on an EASY-nLC II

coupled to an LTQ Orbitrap Velos using a non-linear binary 76 min gradient from 5 – 75 % buffer B (0.1 % acetic acid in acetonitrile) at a flow rate of 300 nL/min and infused into an LTQ Orbitrap Velos (Thermo Fisher Scientific, USA) mass spectrometer. Survey scans were recorded in the Orbitrap at a resolution of 60,000 in the m/z range of 300 – 1,700. The 20 most-intense peaks were selected for CID fragmentation in the LTQ. Dynamic exclusion of precursor ions was set to 20 seconds; single-charged ions and ions with unknown charge were excluded from fragmentation; internal calibration was applied (lock mass 445.120025). For protein identification resulting MS/MS spectra were researched against a database containing protein sequences of *Granulicella* sp. strain WH15 and common laboratory contaminants (9,236 entries) using Sorcerer-Sequest v.27, rev. 11 (Thermo Scientific) and Scaffold v4.8.4 (Proteome Software, USA) as described earlier (Stopnisek *et al.*, 2016). Relative quantification of proteins is based on normalized spectrum abundance factors (NSAF; (Zhang *et al.*, 2010)). The mass spectrometry proteomics data have been deposited to the ProteomeXchange Consortium via the PRIDE (Perez-Riverol *et al.*, 2019) partner repository with the dataset identifier PXD015715. Statistical analysis was done using MeV (Saeed *et al.*, 2003); t-test was applied for proteins that were identified in at least two replicates of the respective condition. Hierarchical clustering and t-test of z-transformed normalized data were performed with the following parameters: unequal group variances were assumed (Welch approximation), P-values based on all permutations with P=0.01, significance determined by adjusted Bonferroni correction. Only significantly changed proteins showing at least two-fold changes between conditions were considered for further analysis. Furthermore, so-called on/off proteins, that were only identified in one condition were analysed. Functional classification of *Granulicella* sp. strain WH15 proteins was carried out using ProPhane software ([www.prophane.de](http://www.prophane.de); (Schneider *et al.*, 2011)), COG (Galperin *et al.*, 2015) and KEGG databases (Kanehisa, 2000). Voronoi treemaps were generated with Paver software (Decodon GmbH, Germany).

### 3. Results

#### 3.1. Genome annotation and CAZymes

The assembled genome of *Granulicella* sp. WH15 is 4,675,153 bp, with 60.7% GC content, 3,849 proteins and only one rRNA operon. Functional annotation using COG (Cluster of Ortholog Groups) and RAST analyses resulted in the classification of 2,620 genes into 23 COG functional groups and the annotation of 1,456 genes to RAST subsystems. The properties and distribution of genes into COGs/RAST functional categories are listed in Table 1 and Figure 1, respectively. A circular genome map of WH15 is depicted in Figure 2.

Table 1. Genomic statistics from *Granulicella* sp. WH15 genome.

Genome	<i>Granulicella</i> sp. WH15
Size (bp)	4,673,153
G+C content (%)	60.7
Number of coding sequences	3,939
Number of features in Subsystems	1,456
Number of RNA genes	51
Number of contigs	1

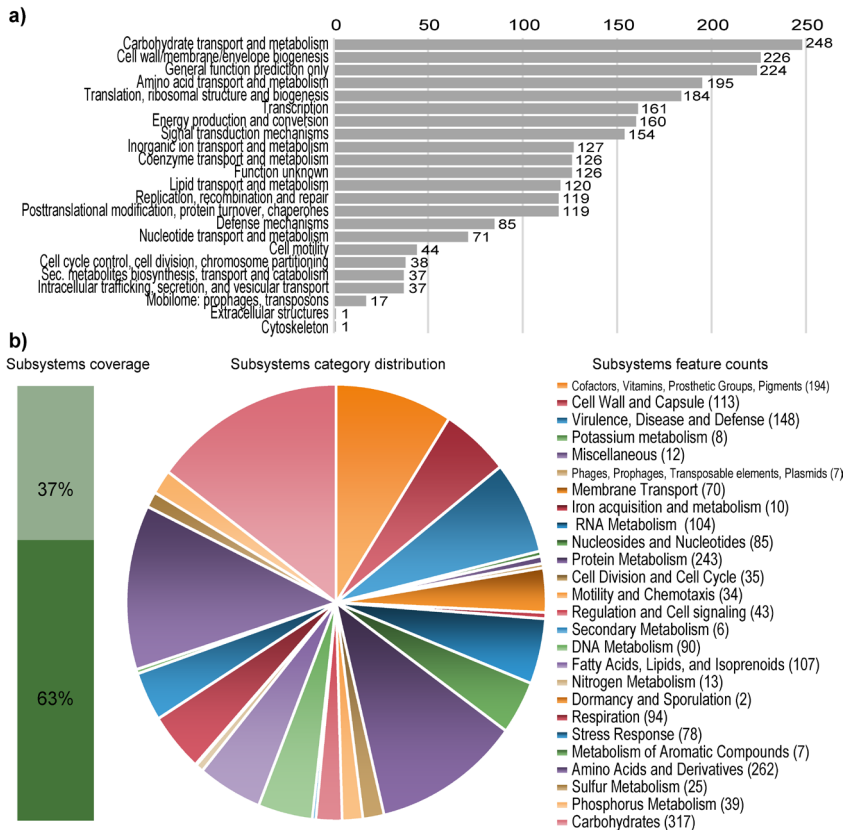


**Figure 1:** Statistics of the COG and RAST subsystem annotations of *Granulicella* sp. WH15. a) COG category distribution showing the number of genes annotated in each category. b) Subsystem category distribution. The light green bar represents the percentage of proteins that could be annotated by the RAST Server, and the dark green bar represents the proteins that were not annotated. The pie chart represents the percentage of proteins annotated to each subsystem category.

RAST analysis showed that only 37% (1456/3939) of the annotated genes were assigned to subsystems. Among the subsystem categories present in the genome, carbohydrates and dormancy and sporulation had the highest and lowest feature counts, respectively (Figure 1). A comparison with five publicly available genomes of *Granulicella* strains showed that the

genome of strain WH15 is larger only than that of *G. pectinivorans* (Table 2). We also performed automatic annotation followed by manual curation of carbohydrate-active enzymes (CAZymes) by using a dbCAN2 search, which revealed 217 CAZyme genes in the strain WH15 genome (E-value  $<10^{-05}$ ) (Table 3). This value is similar to that of other soil *Acidobacteria* Gp1 species determined using the same parameters (Eichorst *et al.*, 2018). Our annotation revealed a poor gene apparatus of strain WH15 for pectin degradation, in contrast to most sequenced soil isolates of *Acidobacteria*. Based on the presence of polygalacturonase genes (GH28), strain WH15 might be capable of breaching the complex heteropolysaccharides of pectins but lacks key genes for breaking the pectin backbone (PL1 and PL4), genes targeting D-xylose substitutions and side chains (GH53, GH54, GH93 and GH127) or genes for further pectin saccharification (GH88 and GH105).

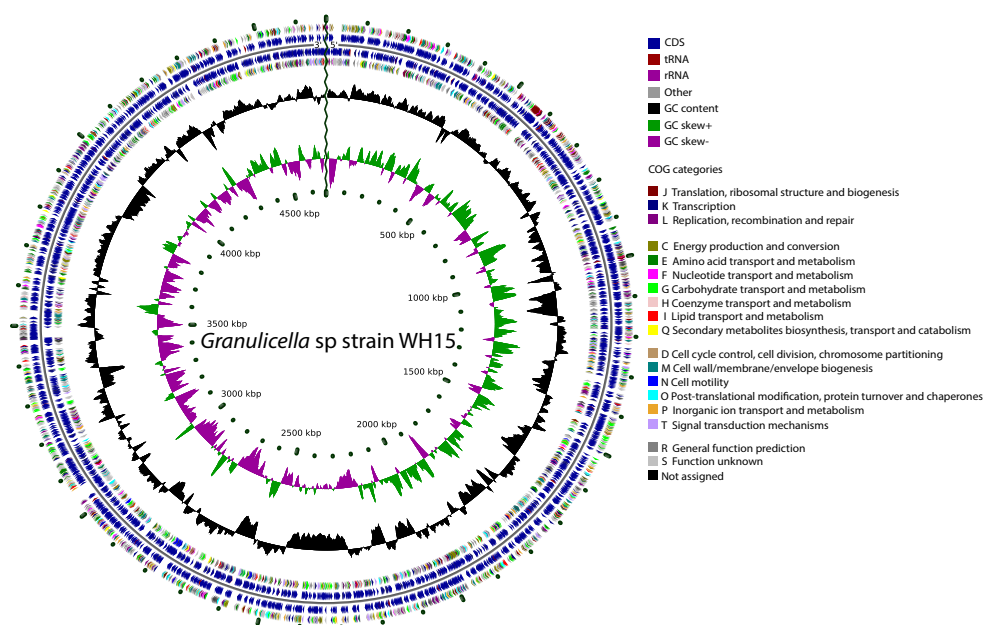


**Figure 2:** Graphical circular genome map of *Granulicella* sp. WH15. The rings indicate coding sequences, COG categories, GC content and GC skew.

Table 2: Comparison of coding sequences, RNA and subsystems among *Granulicella* species with complete genomes sequences available at NCBI.

Genome	Size (bp)	G+C content	Number of coding sequences	Number of features	Number of subsystems	Number of RNAs
<i>Granulicella</i> spp. WH15	4,673,153	60.7	3871	1496	374	51
<i>Granulicella pectinivorans</i> <sup>2</sup>	4,439,413	61.2	3681	1066	302	41
<i>Granulicella mallensis</i> MP5ACTX8 <sup>2</sup>	6,237,577	57.9	5008	1662	394	50
<i>Granulicella tundricola</i> MP5ACTX9 <sup>3</sup>	5,503,984	60	4730	1526	361	49
<i>Granulicella rosea</i> DSM 18704 <sup>1</sup>	5,293,785	62.9	4515	864	250	55

<sup>1</sup>:(Pankratov & Dedysh, 2010); <sup>2</sup>:(Rawat *et al.*, 2013); <sup>3</sup>:(Rawat *et al.*, 2013).

Table 3: CAZYme families observed in the genome of *Granulicella* sp. strain WH15.

CAZYme family	Counts
Auxiliary activity (AA)	13
Carbohydrate binding module (CBM)	22
Carbohydrate esterase (CE)	41
Cohesin	1
Glycoside hydrolase (GH)	86
Glycosyl transferase (GT)	52
Polyssacharide lyase (PL)	2
<b>Total</b>	<b>217</b>

Accordingly, we did not observe growth of strain WH15 on media supplemented with pectin or galacturonic acid, but growth was obtained on media containing sucrose, glucose, cellobiose, xylose, arabinose, mannose, rhamnose, galactose, or lactose (Table S1). These results are consistent with the presence of  $\alpha$ -L-rhamnosidase and  $\beta$ -galactosidase genes in the WH15 genome. In addition, WH15 genome contained *acsC*, *acsAB* and *bcsC*, genes involved in cellulose biosynthesis.

Analysis with the ANTISMASH 4.2.0 database revealed the presence of 33 biosynthetic gene clusters, including 11 of defined type (Table 4) and 22 classified as putative (not shown). Among the putative clusters, 2 have similarities with known clusters involved in the production of O-antigen and thuggacin (Table 4). In addition, other identified clusters showed potential for the production of terpenes, bacteriocins, polyketide synthases (PKS), fatty acids, lasso peptides and saccharides.

Table 4: Biosynthetic gene clusters in the genome of *Granulicella* sp. WH15 revealed by analysis with ANTISMASH.

Cluster	Type	Most similar known cluster
Cluster2	putative	O-antigen BGC (19% of genes show similarity)
Cluster 3	Cf saccharide	
Cluster4	t3pks-cf fatty acid	
cluster 7	Cf saccharide	
cluster 11	lassopeptide	
cluster 13	bacteriocin	
cluster 16	Cf saccharide	
cluster 17	Cf fatty acid-terpene	Malleobactin BGC 11% of genes show similarity)
cluster 19	t3pks	
cluster 22	terpene	
cluster 26	bacteriocin	
cluster 27	Cf saccharide	
Cluster 28	putative	Thuggacin BGC (15% of genes show similarity)

### 3.2. Transcriptome analysis

The total numbers of reads in the low and high cellobiose conditions are listed in Table S2. In total, 106 (53 upregulated and 53 downregulated) genes were significantly differentially expressed ( $p$ -value  $< 0.05$ ) in both treatments, of which only 44 could be annotated, reflecting current gaps in knowledge of the genomes of Acidobacteria in general. Gene expression analysis of *Granulicella* sp. WH15 grown in low and high cellobiose conditions showed that 28 genes were upregulated at  $\log_2 > 1.0$ -fold in the high cellobiose treatment, of which 17 were induced at  $\log_2 > 1.5$ -fold (Table S3). In addition, 30 genes were downregulated at  $\log_2 > 1.0$ -fold in the high cellobiose treatment, of which 12 were repressed at  $\log_2 > 1.5$ -fold (Figure 3) (Table S3). The comparison between the treatments demonstrated that the high cellobiose condition mainly induced the expression of genes related to stress, as well as several unknown hypothetical proteins. Among the annotated genes, a transfer RNA (tRNA-Asn-GTT) was the most upregulated (2.7-fold). In addition, the expression of the genes *gfo4* (glucose-fructose oxidase), tRNA-Asp (GTC), *higA* (HigA antitoxin) and *lytR* (sensory transduction protein LytR) was upregulated ( $> 1.5$ -fold) in the high cellobiose condition, and the expression of genes coding for the stress response sigma factor SigW ( $\sigma^W$ ), peroxiredoxin TsaA and toxin HigB-1 was upregulated  $> 1.0$ -fold. By contrast, the high cellobiose condition suppressed the expression of genes related to cell cycle/division and energy metabolism. Downregulation of expression ( $< 1.5$ -fold) was observed for the genes *trpF* (N-(5'-phosphoribosyl) anthranilate isomerase) and *ssrA* (transfer-messenger RNA), which are involved in amino acid/protein synthesis; two copies of *xerC* (tyrosine recombinase XerC) and the 16S ribosomal RNA gene, which are involved in cell division; *tpiA* (triosephosphate isomerase) and *glpF* (glycerol uptake facilitator protein), which are involved in carbohydrate transport/metabolism; and *hspA* (spore protein SP21), a heat shock chaperone. The expression of genes encoding the housekeeping sigma factor RpoD, 6-phosphogluconate dehydrogenase (*gndA*), RNase P and Lon protease 2 (*lon2*) was also significantly downregulated ( $> 1.0$ -fold). COG category

assignments of the differentially expressed transcripts are presented in Figure 4a. All of the significantly up- and downregulated genes (>1.0 fold) and their annotations are described in Table S3. Among the upregulated transcripts, two genes could be assigned to KEGG pathways: *tsaA* (K11188 - metabolic pathways, biosynthesis of secondary metabolites and phenylpropanoid biosynthesis) and *lytR* (K07705 - two-component system) (Figure 4a). Of the downregulated transcripts, 5 genes were linked to metabolic pathways in the KEGG database: *trpF* (5 pathways), *tpiA* (10 pathways), *dnaK* (1 pathway), *trpC* (5 pathways) and *gndA* (8 pathways) (Figure 4b). These genes are mostly related to the production of antibiotics and secondary metabolites, as well as amino acid and carbon metabolism. The metabolic pathways for each gene are described in Table 5.

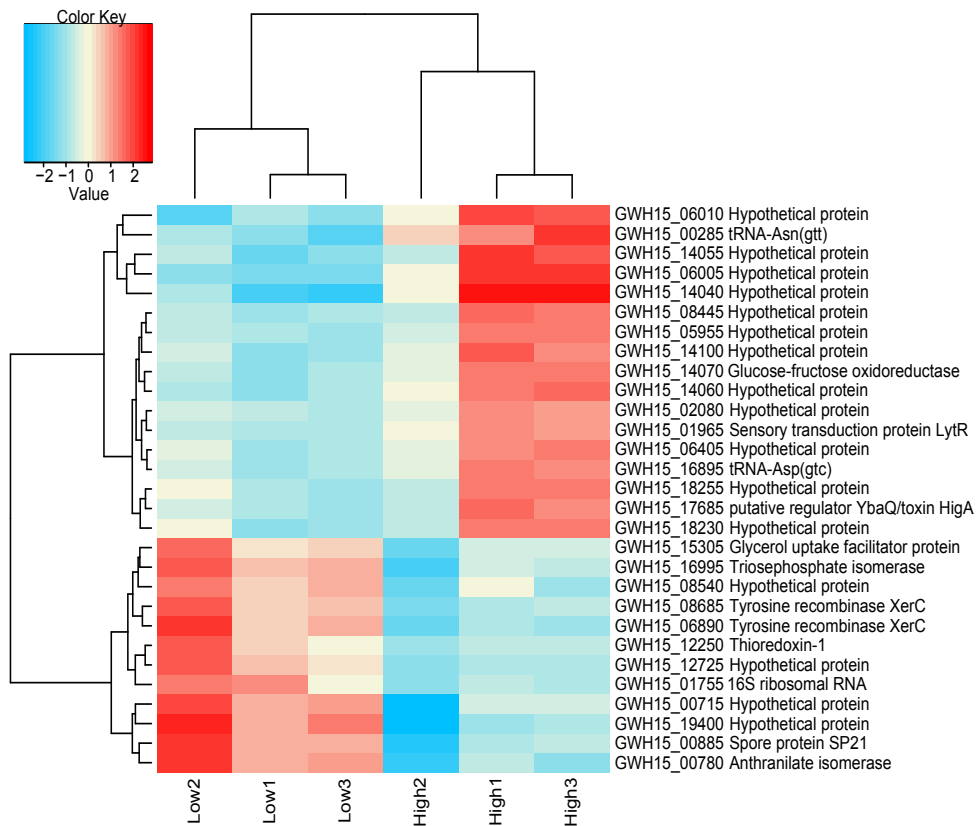


**Figure 3:** Heatmap of transcriptome data from *Granulicella* sp. WH15 showing the top differentially expressed genes ( $\log_2 > 1.5$ -fold) and hierarchical clustering analysis in high cellobiose versus low cellobiose concentrations. High to low expression is shown by a gradient color from red to blue, respectively. Low – 0.025% cellobiose concentration. High – 3% high cellobiose concentration. Differentially expressed genes between the two treatments, using low cellobiose treatment as a reference, were identified at significance level of 0.05 with a false discovery rate (FDR) correction method. Each treatment had three replicates.

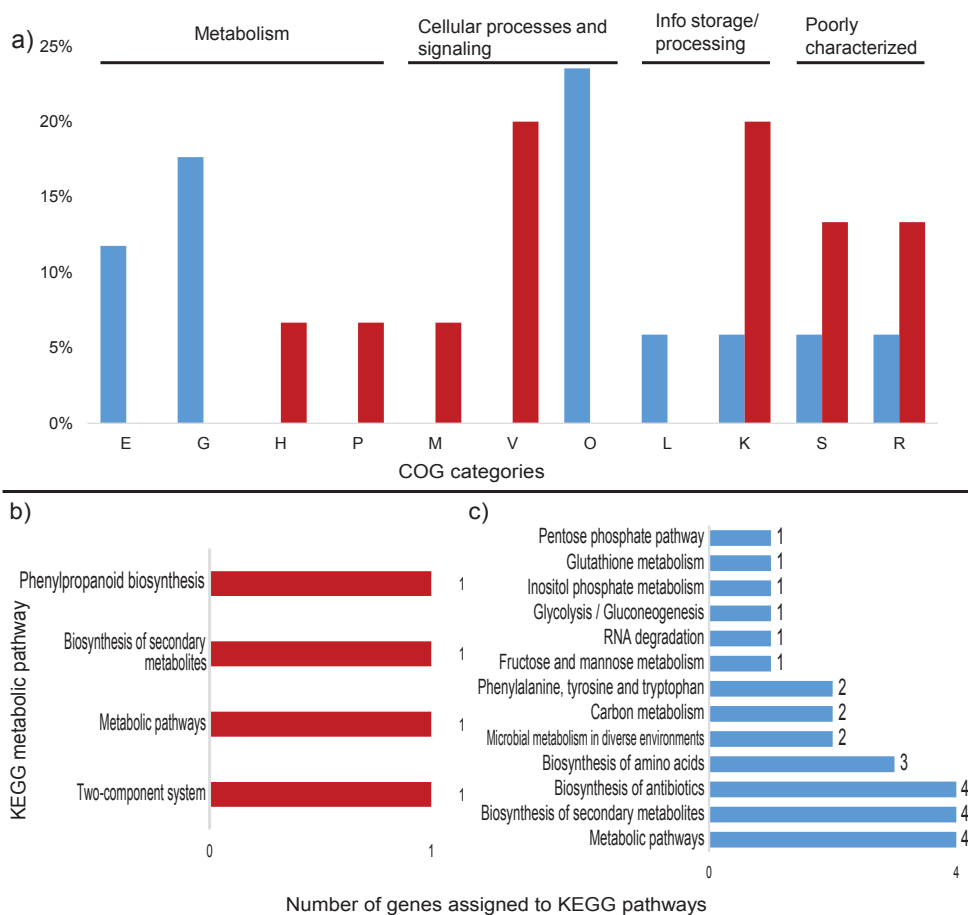


**Figure 4:** Differentially expressed transcripts assigned to COG categories and KEGG pathways in the transcriptomic profile of *Granulicella* strain WH15, up- and downregulated in high cellobiose treatment. a) Percentage of upregulated (red) and downregulated (blue) transcripts assigned to COG categories; b) Number of upregulated transcripts assigned to KEGG pathways c) Number of downregulated transcripts assigned to KEGG pathways. Unassigned transcripts are not shown. E-Amino acid transport and metabolism; G- Carbohydrate transport and metabolism; H-Coenzyme transport and metabolism; M-Cell wall/membrane/envelope biogenesis; V-Defense mechanisms; P-Inorganic ion transport and metabolism; O-Post-translational modification; L-Replication, recombination and repair; K-Transcription; S-Function unknown; R-General function and prediction.

Table 5: KEGG metabolic pathways assigned to significantly downregulated genes of *Granulicella* sp WH15 in high cellobiose treatment.

KEGG orthology	Gene	Related KEGG pathways
K01817	<i>trpF</i>	Biosynthesis of antibiotics, secondary metabolites and aminoacids; metabolic pathways; phenylalanine, tyrosine and tryptophan biosynthesis.
K01803	<i>tpiA</i>	Biosynthesis of antibiotics, secondary metabolites and aminoacids; metabolic pathways; phenylalanine, tyrosine and tryptophan biosynthesis; microbial metabolism in diverse environments; carbon metabolism; inositol phosphate metabolism; fructose and mannose metabolism; glycolysis / gluconeogenesis.
K04043	<i>dnaK</i>	Genetic information processing-folding, sorting and degradation.
K01609	<i>trpC</i>	Biosynthesis of antibiotics, secondary metabolites and aminoacids; metabolic pathways; phenylalanine, tyrosine and tryptophan biosynthesis.
K00033	<i>gndA</i>	Biosynthesis of antibiotics and secondary metabolites; Metabolic pathways; microbial metabolism in diverse environments; carbon metabolism; phenylalanine, tyrosine and tryptophan biosynthesis; glutathione metabolism; pentose phosphate pathway.

### 3.3. Proteome analysis

Qualitative analysis of the proteomic data demonstrated that the samples clustered according to treatment, i.e., high or low cellobiose condition (Figure S1). In total, 1,418 proteins could be identified in both conditions in two of three replicates each. Overall, 448 proteins showed significant differences between the low and high cellobiose conditions (t-test,  $p=0.01$ ; Figure S2). In addition, 249 so-called on/off proteins that were only present in one condition were detected. The proteome patterns of WH15 under the low and high cellobiose treatments are depicted in Figure 5. In the high cellobiose condition, 121 proteins were upregulated two-fold, and 129 proteins were “on”; 78 proteins were downregulated at least twofold, and 120 proteins were “off” (Figure 5; Tables S4 and S5). A comparison with the transcriptome data revealed that 2 ORFs (*lytR* and a hypothetical protein – ORF 05985) were upregulated, and 2 ORFs (*gndA* and a hypothetical protein – ORF 08600) were downregulated in both datasets for the high cellobiose treatment. Among the differentially expressed proteins, 332 could be assigned to COG categories, and 184 were annotated to KEGG orthologs (Figure 6).

#### 3.3.1. Upregulated proteins

COG analysis demonstrated that most of the upregulated proteins belong to the categories cell wall/membrane/envelope biogenesis (44) and defense mechanism (16) (Figure 6a). TigrFam classification grouped most of the upregulated/on proteins in the categories protein fate (27), followed by cellular processes (21), transport/binding proteins (20) and cell wall/membrane/envelope biogenesis (12) (Figure S3). Closer examination of the subroles of the most abundant protein categories demonstrated that their main functions were related to peptide secretion and trafficking, detoxification and toxin production/resistance processes, efflux pumps, transporters and TonB-dependent receptors (Table S4). In addition to the sensory transduction protein *LytR* (*lytR*), which was also upregulated in the transcriptome data, several cell membrane proteins could be identified, such as the outer membrane protein *OprM* (*oprM* 1,4, 5, 6 and 7), the LPS-assembly protein *LptD* (*lptD* 2), the macrolide

export proteins MacA and MacB (*macA* 1, *macB* 6 and 8), the polysialic acid transport protein KpsD (*kpsD* 2) and the multidrug resistance proteins MdtB and MdtC (*mdtB* 2 and 3, *mdtC* 3 and 6). Among the upregulated proteins, 135 were annotated to KEGG orthologs, but only 44 orthologs could be mapped to KEGG metabolic pathways (Figure 6b, Table S6), and some identifiers were assigned to more than one pathway. Most of the proteins were mapped to ‘general’ metabolic pathways (15), two-component systems (9), biosynthesis of secondary metabolites (6), ABC transporters (4) and bacterial secretion systems (4), indicating that no particular metabolic pathway seemed to be specifically stimulated under the high cellobiose condition (Figure S4), although the expression of many membrane proteins was enhanced (Figure 7). However, when the genes assigned to the COG carbohydrate transport and metabolism category were examined, proteins related to trehalose metabolism were observed, such as OtsA (trehalose-6-phosphate synthase), TreS (trehalose synthase) and GlgE 1 (alpha-1,4-glucan:maltose-1-phosphate maltosyltransferase), as well as a hypothetical protein similar to cellobiose phosphorylase (ORF GWH15\_11910). Another interesting protein identified was CcpA (catabolite control protein A) (Table S4), which is involved mainly in carbon

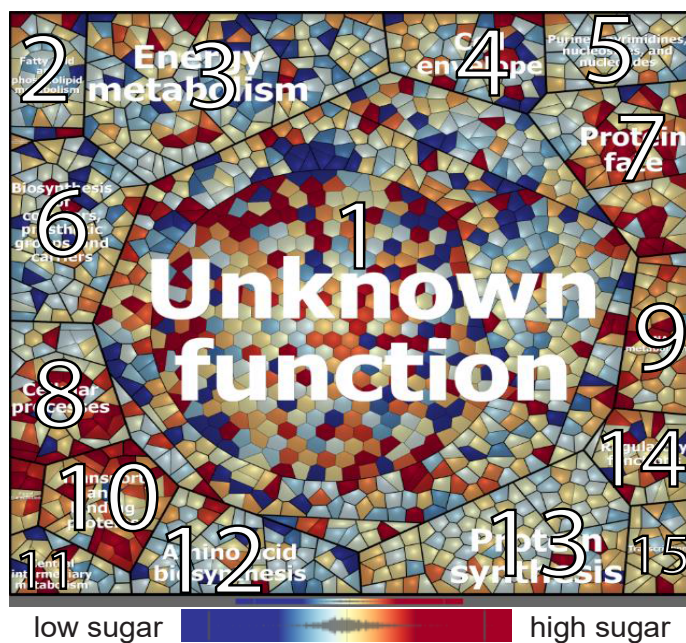


**Figure 5:** Voronoi treemap visualization of the protein expression patterns of *Granulicella* sp. WH15 under low and high cellobiose concentrations. Functional classification was conducted using Prophane 2.0 ([www.prophane.de](http://www.prophane.de)) and is based on TIGRFAMS, function level “main role“. Each cell represents a quantified protein; proteins are clustered according to their function. Proteins with higher amount under low cellobiose conditions are depicted in blue, proteins with higher amount in high cellobiose conditions are depicted in red. 1- unknown function; 2-fatty acid and phospholipid metabolism; 3-energy metabolism; 4-cell envelope; 5-nucleotide metabolism; 6-co-factors and prosthetic groups; 7-protein fate; 8-cellular processes; 9-DNA metabolism; 10-transport and binding proteins; 11-central intermediary metabolism; 12-aminoacid biosynthesis; 13-protein synthesis; 14-regulatory functions; 15-transcription.

metabolism regulation (Fujita, 2014).

### 3.3.2. Downregulated proteins

Within the COG categories, the downregulated proteins were mostly distributed among the carbohydrate transport and metabolism (35), amino acid transport and metabolism (20) and

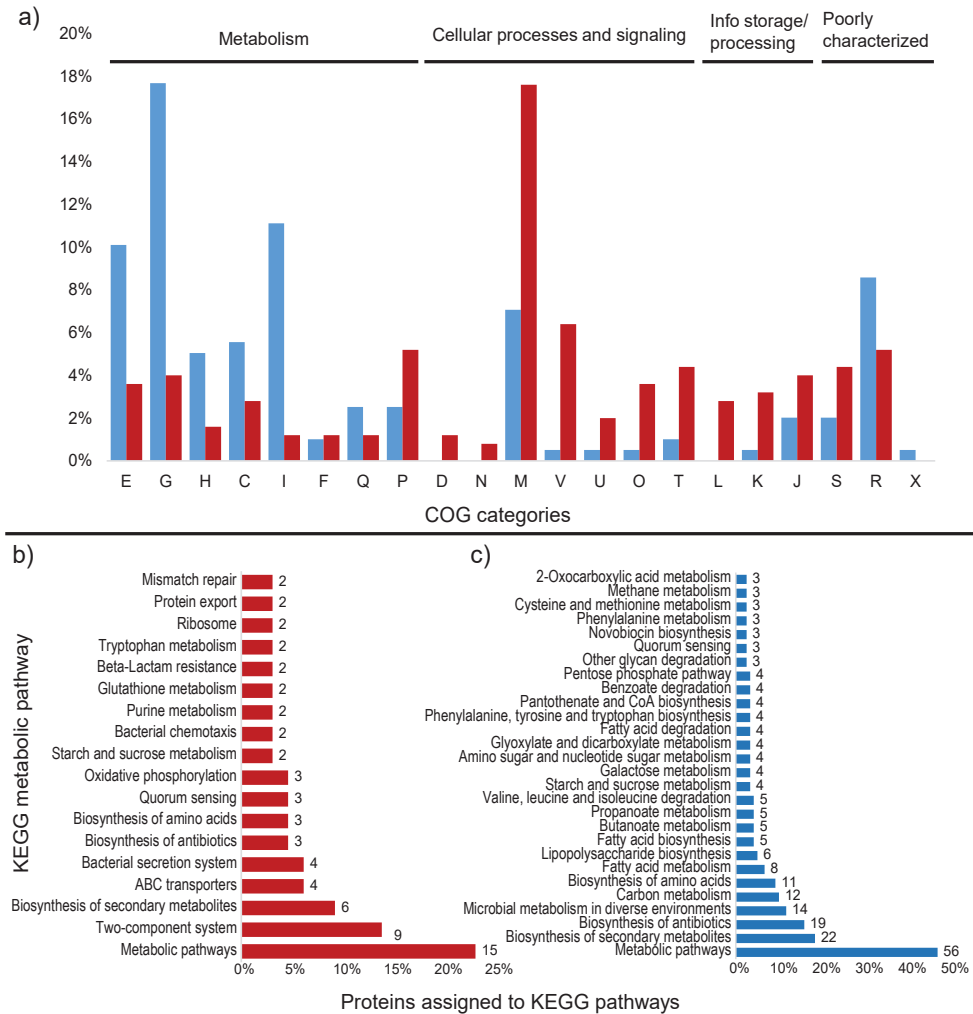


**Figure 6:** Differentially expressed proteins assigned to COG categories and KEGG pathways in the proteomic profile of *Granulicella* strain WH15 in high cellobiose concentration. a) Percentage of upregulated (red) and downregulated (blue) proteins assigned to COG categories; b) Percentage and number of upregulated proteins assigned to KEGG pathways; c) Percentage and number of downregulated proteins assigned to KEGG pathways. Unassigned proteins are not shown. E-Amino acid transport and metabolism; G-Carbohydrate transport and metabolism; H-Coenzyme transport and metabolism; C-Energy production and conversion; I-Lipid transport and metabolism; F-Nucleotide transport and metabolism; Q-Secondary metabolites; D-Cell cycle; N-Cell motility; M-Cell wall/membrane/envelope biogenesis; V-Defense mechanisms; P-Inorganic ion transport and metabolism; U-Intracellular trafficking; O-Post-translational modification; T-Signal transduction mechanisms; L-Replication, recombination and repair; K-Transcription; J-Translation; S-Function unknown; R-General function and prediction; X-Mobilome.

lipid transport and metabolism (22) categories (Figure 6a). TigrFam classified most of the downregulated/off proteins in the categories of energy metabolism (29) and biosynthesis of cofactors, prosthetic groups and carriers (13) (Figure S3). Among the TigrFam subroles of the most abundant categories, most of the proteins were related to sugar metabolism and biosynthesis of vitamins. In total, 119 proteins were assigned to KEGG orthologs, and 68 orthologs were assigned to KEGG metabolic pathways. The majority of the proteins were assigned to ‘general’ metabolic pathways (56), biosynthesis of secondary metabolites (22), biosynthesis of antibiotics (19), microbial metabolism in diverse environments (12), carbon metabolism (12) and biosynthesis of amino acids (11) (Figure 6b). Consistent with the COG categories, downregulation of proteins linked to KEGG pathways involved in carbon, amino acid and lipid metabolism was observed (Figure S4, Table S5). In addition to general carbon metabolism, pathways related to secondary carbon sources seemed to be repressed, such as the metabolism of starch, sucrose, galactose, amino sugars, nucleotide sugars, fructose, mannose and other glycans, the pentose phosphate pathway, and glycolysis (Figure 6b, Figure 7, Table S6). Repression of pathways related to several amino acids, such as valine, leucine, phenylalanine, tyrosine and tryptophan, and the metabolism of fatty acids and lipopolysaccharides was observed (Figure 6b). The carbon-related repressed proteins

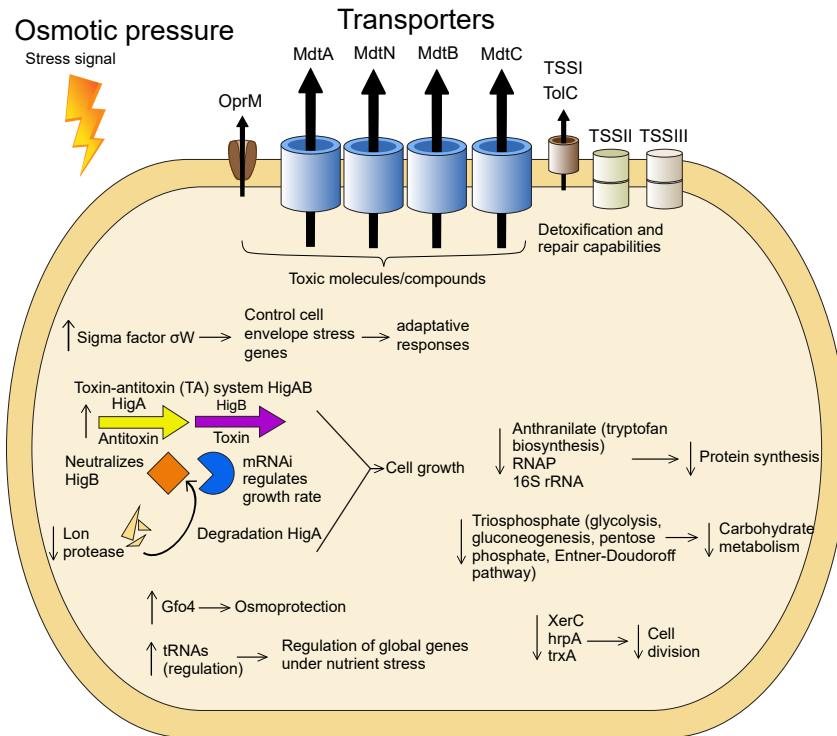


**Figure 7:** Model of the cellular processes involved in the adaptation to higher concentrations of cellobiose in *Granulicella* sp. WH15. The arrows depict upregulation (↑) and downregulation (↓) of transcripts and proteins.

included beta galactosidases (BgaA and BgaB), 1,4-beta-D-glucan glucohydrolase (GghA), xylan 1,4-beta-xylosidase (Xyl3A 1), beta-xylosidase (XynB), endopolygalacturonase (PehA 1), and exo-poly-alpha-D-galacturonosidase (PehX). Furthermore, 4 enzymes involved in the pentose phosphate pathway were downregulated: 6-phosphogluconate dehydrogenase, NADP (+)-dependent decarboxylase (GndA), transketolase 2 (TktB 1), gluconolactonase (Gnl 1) and KHG/KDPG aldolase (Eda). Among the proteins related to amino acid metabolism, the glutamate-pyruvate aminotransferase AlaA (alanine), histidinol-phosphate aminotransferase HisC2 (histidine), and prephenate dehydrogenase TyrA2 (tyrosine) were repressed. Enzymes involved in fatty acid degradation such as 3-ketoacyl-CoA thiolase (FadA), acyl-CoA dehydrogenase (FadE) and 3-hydroxyacyl-CoA dehydrogenase (FadN) were also downregulated (Table S5).

#### 4. Discussion

*Granulicella* sp. WH15, an isolate collected from soil containing decaying wood, has a genome of 4.7 Mbp. Genome analysis revealed that a large number of genes were assigned to subsystem categories of carbohydrates (14.8%), amino acids and derivatives (12.2%) and protein metabolism (11.3%). Among other strains of *Granulicella*, 6.9% of the *G. tundricola* MP5ACTX9<sup>T</sup> genome (Rawat *et al.*, 2013) and 9.1% of the *G. mallensis* MP5ACTX8<sup>T</sup> genome (Rawat *et al.*, 2013) are dedicated to the transport and metabolism of carbohydrates. Similar to other *Granulicella* strains, strain WH15 possesses a wide range of glycoside hydrolases suggesting that this bacterium is well equipped for the carbon cycling process in soil as well as the hydrolysis and utilization of stored carbohydrates and the biosynthesis of exopolymers (Rawat *et al.*, 2013, Rawat *et al.*, 2013). The saccharide gene clusters revealed by ANTISMASH analysis are likely involved in the production of capsule, antigen and exopolymers. Exopolymer production by this strain has been observed under laboratory conditions, and the composition of the biopolymer has been characterized (Kielak *et al.*, 2017). However, the expression of gene clusters and proteins related to the production of EPS was not observed in this study, as the timepoint of cell collection was too early for substantial EPS production, which primarily occurs in stationary phase for both strains (Kielak *et al.*, 2017).

Members of the phylum *Acidobacteria* are generally considered slow-growing organisms that succeed in oligotrophic environments. The acidobacterium *Granulicella* sp. was isolated by employing a low nutrient culture medium (Valášková *et al.*, 2009), similar to other strains of *Granulicella* (Pankratov & Dedysh, 2010, Mannisto *et al.*, 2012). Although this strain can be cultivated using low quantities of nutrients, it also develops well in higher concentrations of sugar (Campanharo *et al.*, 2016). To better understand the behavior of *Granulicella* sp. WH15 in response to different carbon source concentrations, comparative transcriptomic and proteomic analyses were performed under 0.025% and 3% cellobiose. We used the low

cellobiose concentration as a reference, therefore evaluating up and downregulated proteins in the high cellobiose treatment. The comparative transcriptomic and proteomic profiles of strain WH15 under low and high cellobiose conditions demonstrated that the higher concentration of cellobiose triggered the expression of transcripts and proteins related to stress responses. These results suggest that the higher cellobiose concentration might have generated an osmotic stress condition for our strains. Stress conditions in bacteria induce changes at the transcriptional level that are often associated with a variety of  $\sigma$  factors, which bind to RNA polymerase (Helmann, 2016). Transcriptomic profiling showed that, in addition to other stress proteins, the sigma factor  $\sigma^W$  was upregulated  $\log_2 > 1.0$ -fold. In *Bacillus subtilis*, the  $\sigma^W$  regulon controls genes related to cell envelope stress, membrane proteins and proteins involved in protection against toxins or antibiotics. Expression of this regulon has been observed under conditions of stress that affect cell wall biosynthesis or membrane integrity, such as alkali shock, salt stress, and treatments with cationic peptides and detergents (Zweers *et al.*, 2012). The cell envelope is the most external form of bacterial defense and receives stress stimuli, senses perturbations, and transmits signals that induce the transcriptional changes necessary for an adaptive response (Sacheti *et al.*, 2014). Another stress system upregulated in the high cellobiose condition was the toxin-antitoxin (TA) system HigAB. The prokaryotic TA system encodes a stable toxin (HigB) and an unstable antitoxin (HigA) that neutralizes HigB. HigB is an mRNA interferase that is believed to be involved in growth rate control (Christensen-Dalsgaard *et al.*, 2010). Expression of the system is induced by various stress stimuli, such as nutritional stress, heat shock (Tachdjian & Kelly, 2006), and exposure to chloramphenicol and chloroform (Gvakharia *et al.*, 2007, Jorgensen *et al.*, 2008). In *Escherichia coli*, amino acid starvation strongly induces the transcription of the TA system (Christensen-Dalsgaard *et al.*, 2010). The higher expression level of the antitoxin HigA compared to HigB in this study suggests that the acidobacterial cells were adapting to stress (Hayes & Low, 2009) and therefore produced more antitoxin to counterbalance the effect of HigB. In addition, these results are compatible with the downregulation of Lon protease, which contributes to the proteolytic regulation of many cell functions and is involved in the degradation of HigA (Christensen *et al.*, 2001).

The upregulated gene *gfo4* encodes glucose-fructose oxidoreductase, an enzyme involved in the production of molecules that function in intracellular osmoprotection under high cellobiose conditions (Nidetzky *et al.*, 1997). The production of this enzyme could be important to counterbalance the effects of the higher amounts of cellobiose in the culture medium. By contrast, the gene *glpF*, which encodes a glycerol uptake facilitator protein, was downregulated. This aquaglyceroporin facilitates the transport of glycerol and other linear polyalcohols across membranes, which would be redundant, as the cell is able to produce such molecules via the glucose-fructose oxidoreductase *gfo4*.

Another upregulated protein, LytR, is a sensory transduction protein that is part of the LytSR system, which in *Staphylococcus aureus* functions as a sensor-response system that detects

perturbations in the electrical potential of the cell membrane, such as disturbances caused by the presence of stress agents (Patel & Golemi-Kotra, 2016). Furthermore, the upregulation of tRNA genes could be involved in expression regulation. In addition to their central role in protein synthesis, tRNAs are involved in the regulation of global gene expression during nutritional stresses to adapt microbial metabolism to changes in amino acid concentrations (Li & Zhou, 2009). In the yeast *Saccharomyces cerevisiae*, for instance, glutamine tRNA is responsible for sensing of nitrogen sources in the environment and acts as a development regulator (Murray *et al.*, 1998). In addition, under different stress conditions, the relative abundances of tRNAs in *S. cerevisiae* change towards tRNAs recognizing rare codons to induce faster translation of the stress proteins necessary for adaptation (Torrent *et al.*, 2018). Although these functions of tRNAs were described in yeast, similar functions may be present in bacteria such as strain WH15.

The proteomic profile of the high cellobiose treatment was consistent with the upregulation of stress-related genes observed in the transcriptomic analyses. Most of the upregulated/on proteins were membrane proteins related to peptide secretion and trafficking, detoxification and toxin resistance, efflux pumps and transporters, and cell wall and defense mechanisms. The high abundance of membrane proteins may indicate the increased production of toxic metabolites, which can be removed from cells via pump systems (Rosner & Martin, 2009). The upregulated membrane transporters included type I (TolC family), II and III secretion system proteins, the multidrug resistance proteins MdtA, MdtN, MdtB and MdtC, and the outer membrane protein OprM. The protein TolC is important for membrane structure and function in *E. coli*, as well as in the export of toxic molecules in gram-negative bacteria, and TolC mutants are impaired in detoxification and repair (Zgurskaya *et al.*, 2011). The proteins MdtA, MdtN, MdtB and MdtC belong to the resistance-nodulation-division (RND) family of transporters, which play a role in drug resistance in gram-negative bacteria and promote the efflux of a wide range of toxic compounds, including antibiotics and detergents (Nikaïdo, 1996, Kim *et al.*, 2009). The outer membrane protein OprM is part of a membrane protein complex capable of actively ejecting an assortment of harmful compounds and is most notably involved in multidrug-resistance in gram-negative bacteria such as *Pseudomonas aeruginosa* (Federici *et al.*, 2005). Interestingly, genes encoding cation/multidrug efflux pumps are upregulated in cells of *Acetobacter aceti* grown in glucose, although the reasons are unknown (Sakurai *et al.*, 2010).

KEGG metabolic pathway analysis of the upregulated proteins and transcripts demonstrated that no specific metabolic pathway was enhanced by the high cellobiose treatment. Nonetheless, a predominance of categories related to membrane protein complexes was observed, such as two-component systems, ABC transporters and bacterial secretion systems. Closer examination of the proteins involved in carbon metabolism revealed the upregulation of proteins related to trehalose biosynthesis, such as trehalose-6-phosphate synthase (OtsA), trehalose synthase (TreS) and alpha-1,4-glucan:maltose-1-phosphate maltosyltransferase

(GlgE 1). Trehalose is an osmoprotectant disaccharide that accumulates in microorganisms under conditions of osmotic stress, and its role in cellular protection has been demonstrated in bacteria and yeast (Ruhel *et al.*, 2013). The expression of these enzymes indicates that the bacterial cells were reacting to the high cellobiose conditions by storing trehalose to increase their resistance to osmotic stress conditions.

The upregulation of protein GWH15\_11910, which is similar to a cellobiose phosphorylase, may confirm the use of cellobiose as a carbon source, since this enzyme catalyzes the phosphorolysis of the  $\beta$ -1,4-glucosidic bond of the disaccharide to produce  $\alpha$ -D-glucose-1-phosphate and D-glucose (Bianchetti *et al.*, 2011); however, no other carbon metabolism pathways were enhanced. Furthermore, the catabolic control protein CcpA was upregulated. The impact of this protein on cellular metabolism will be discussed later, as it promotes the repression of several metabolic pathways. The analysis of the downregulated transcripts indicated a decline in cell activity marked by reduced protein synthesis, carbohydrate metabolism and cell division. The downregulated proteins included the enzyme anthranilate isomerase, which is involved in tryptophan biosynthesis (Thoma *et al.*, 2000); RNase P, which is responsible for the production of the mature 5' ends of precursor tRNAs and is essential for translation (Schön, 1999); and the small subunit of the ribosome, 16S rRNA, which is fundamental for protein synthesis in prokaryotes (Singh *et al.*, 2018). As part of central carbon metabolism, the enzyme triosephosphate isomerase is vital for energy production, since it plays a key role in glycolysis, gluconeogenesis, and the pentose phosphate and Entner-Doudoroff pathways (Paterson *et al.*, 2009). The tyrosine recombinase XerC has a significant role in chromosome segregation during cell division and is important for the maintenance of replicon stability in *E. coli* (Grainge & Sherratt, 1999), and the chaperone HspA is a heat shock protein that is involved in the correct folding of proteins (Scieglinska & Krawczyk, 2014). The thioredoxin TrxA is a small redox protein that also possesses a chaperone function (Negrea *et al.*, 2009). The analysis of the downregulated proteins further revealed that the majority of the proteins were related to energy metabolism and cofactor biosynthesis, consistent with the downregulation of transcripts related to carbohydrate metabolism and cell division. Similarly, when exposed to osmotic stress, the metabolism of *E. coli* growing in minimal medium slows, and respiration and macromolecule synthesis are inhibited (Houssin *et al.*, 1991). Osmotic pressure produces deformation of the cell membrane, which could explain the expression of membrane stress signals observed in the present study. In addition, osmotic stress in *Sinorhizobium meliloti* promotes the repression of several functions of central metabolism and energy production systems (Dominguez-Ferreras *et al.*, 2006).

An important protein impacting cell metabolism is the catabolic control protein CcpA, which was upregulated under high cellobiose conditions. This protein is involved in carbon catabolite repression (CCR), a regulatory process that, in the presence of a preferable carbon source, inhibits alternative metabolic pathways (Jankovic & Bruckner, 2002). Although mainly found in Gram-positive bacteria, it has been suggested that Gram-negative bacteria might have

CcpA-dependent CCR (Warner & Lolkema, 2003). CCR regulates not only genes and operons involved in carbon metabolism but also those involved in the metabolism of amino acids and nucleotides and in the synthesis of extracellular enzymes and secondary metabolites (Fujita, 2014). Consistent with this process, we observed the downregulation of several enzymes related to secondary carbon source hydrolysis, such as beta galactosidases, xylosidases and galacturonases, as well as the pentose phosphate (PP) pathway. The PP pathway is fundamental for the generation of NADPH molecules and biosynthetic intermediates that are essential for the production of fatty acids, glutamate, purines, histidine and aromatic amino acids (Richardson *et al.*, 2015). Therefore, downregulation of the PP pathway could also contribute to the general repression of cell metabolism. Furthermore, enzymes related to amino acids, fatty acid metabolism and their corresponding KEGG pathways were repressed. Although many transcripts and proteins could not be identified due to limited information in the databases, the analysis of the present dataset suggested that the addition of a high cellobiose concentration in the culture medium of *Granulicella* sp. WH15 initially triggered a stress response. As part of this response, the expression of excretory membrane proteins was enhanced to promote the secretion of putative toxic byproducts from bacterial metabolism; energy metabolism was repressed to reallocate resources towards maintenance instead of growth; and the production of the osmoprotectant trehalose was enhanced. Data from experiments of bacteria under disturbances are important for understanding the behavior of microorganisms in response to environmental stresses, particularly for *Acidobacteria*, which is highly abundant in soil but whose soil ecology remains to be established. Further studies will improve the understanding of the mechanisms underlying the adjustment of the slow growth of *Granulicella* and other *Acidobacteria* strains to higher growth rates.

## Acknowledgements

We thank Victor de Jager and Mattias de Hollander for bioinformatics assistance, Genomics Resource Center (USA) for the bacteria genome sequencing. This research was supported by (NWO-729.004.013). Ohana Y.A. Costa was supported by an SWB grant from CNPq [202496/2015-5] (Conselho Nacional de Desenvolvimento Científico e Tecnológico).

## Supplementary material

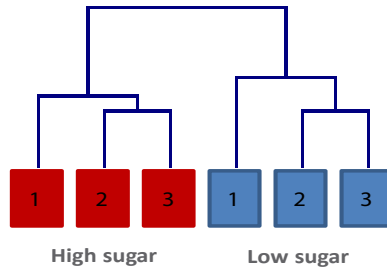


**Figure S1:** Cluster analysis of the proteome profile based on qualitative data in low and high cellobiose conditions. Hierarchical clustering of z-transformed normalized data was performed assuming unequal group variances (Welch approximation) and p-values based on all permutations ( $p=0.01$ ) were adjusted using Bonferroni correction.

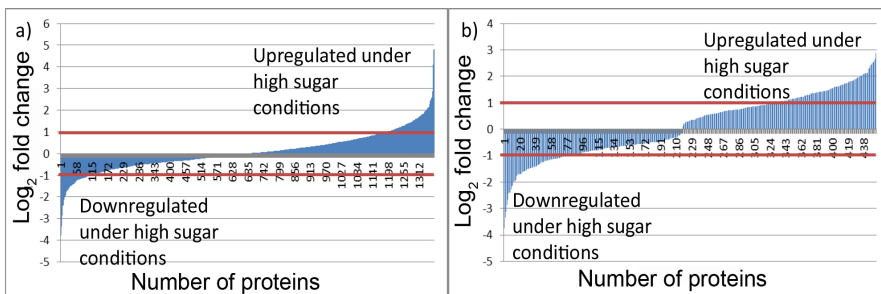


**Figure S2:** Expression pattern of proteins under high and low cellobiose cultivation of *Granulicella* sp. WH15 a) All proteins identified in at least two out of three replicates (excluding on/off proteins). b) Only proteins with significant change t-test  $p=0.01$ .  $\log_2$  fold change is indicated by a red line.

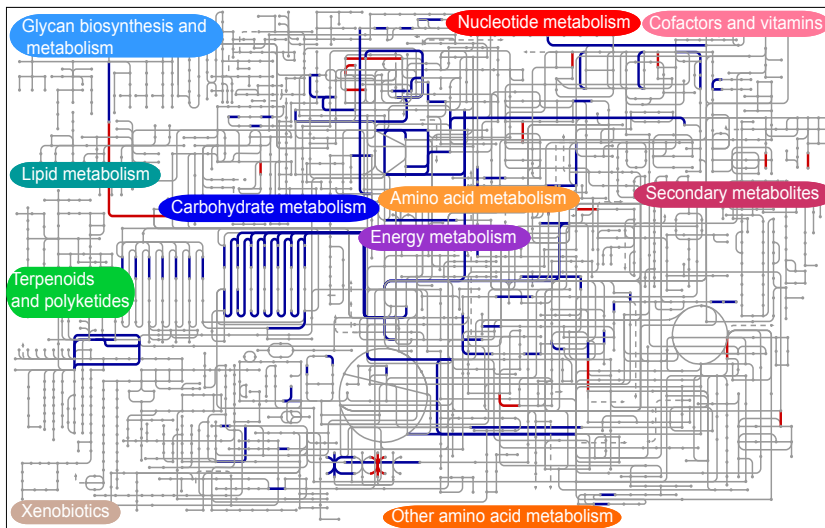


**Figure S3:** General overview of up (red) and downregulated (blue) metabolic pathways based on KEGG analysis of differentially expressed proteins in the proteomic profile of *Granulicella* sp WH15 in high cellobiose concentration. No particular metabolic pathway seemed to be specifically upregulated and downregulated proteins were mostly distributed among the carbohydrate transport and metabolism pathways.

Table S1: Growth of strain *Granulicella* sp. WH15 in culture media supplemented with different carbon sources.

Carbon source	Growth
Pectin	-
Glycogen	-
Glucosamine	-
Cellulose	-
D-glucose	+
D-galactose	+
D-mannose	+
D-xylose	+
L-arabinose	+
L-rhamnose	+
D-galacturonic acid	-
Cellobiose	+
D-lactose	+
Sucrose	+

+=positive growth; -=No growth

3

Table S2. Total number of transcripts reads per sample in the transcriptomic profile of *Granulicella* sp. WH15 under low and high cellobiose concentrations.

Sample ID	Total number of reads
Low cellobiose (1)	15,731,147
Low cellobiose (2)	12,624,878
Low cellobiose (3)	11,080,985
High cellobiose (1)	11,138,128
High cellobiose (2)	9,322,795
High cellobiose (3)	10,071,593

Table S3: Differentially expressed transcripts in the transcriptomic profile of *Granulicella* sp. WH15 in high cellobiose concentration. Only statistically significant differentially expressed genes with a fold change  $\geq 1.0$  or  $\leq -1.0$  are shown.

ORF	Annotation	Log <sub>2</sub> FC
GWH15_14040	hypothetical protein	3.71
GWH15_06005	hypothetical protein	3.12
GWH15_00285	tRNA-Asn(gtt)	2.74
GWH15_06010	hypothetical protein	2.70
GWH15_14055	hypothetical protein	2.66
GWH15_14060	hypothetical protein	2.18
GWH15_14100	hypothetical protein	2.00
GWH15_08445	hypothetical protein	1.94
GWH15_05955	hypothetical protein	1.93
GWH15_14070	gfo4	1.92
GWH15_16895	tRNA-Asp(gtc)	1.72
GWH15_17685	higA	1.71
GWH15_18230	hypothetical protein	1.67
GWH15_01965	lytR	1.67

ORF (continued)	Annotation	Log <sub>2</sub> FC
GWH15_18255	hypothetical protein	1.60
GWH15_06405	hypothetical protein	1.59
GWH15_02080	hypothetical protein	1.54
GWH15_10070	hypothetical protein	1.47
GWH15_07155	hypothetical protein	1.41
GWH15_03690	hypothetical protein	1.37
GWH15_14050	sigW	1.35
GWH15_05960	hypothetical protein	1.32
GWH15_05985	hypothetical protein	1.26
GWH15_17690	higB-1	1.17
GWH15_11830	hypothetical protein	1.13
GWH15_14160	hypothetical protein	1.10
GWH15_06410	hypothetical protein	1.06
GWH15_04600	putative peroxiredoxin	1.04
GWH15_17625	hypothetical protein	-1.03
GWH15_00710	hypothetical protein	-1.06
GWH15_00505	rpoD	-1.09
GWH15_16220	hypothetical protein	-1.19
GWH15_14410	Lon protease 2	-1.20
GWH15_08600	hypothetical protein	-1.21
GWH15_14215	hypothetical protein	-1.22
GWH15_10510	hypothetical protein	-1.29
GWH15_00210	RNaseP_bact_a	-1.30
GWH15_01535	gndA	-1.33
GWH15_00720	hypothetical protein	-1.33
GWH15_01770	23S ribosomal RNA	-1.34
GWH15_19395	hypothetical protein	-1.34
GWH15_00785	trpC	-1.39
GWH15_04765	xerC	-1.44
GWH15_01625	dnaK	-1.45
GWH15_11560	hypothetical protein	-1.47
GWH15_07810	ssrA	-1.53
GWH15_15305	glpF	-1.63
GWH15_08540	hypothetical protein	-1.75
GWH15_12250	trxA	-1.80
GWH15_01755	16S ribosomal RNA	-1.94
GWH15_12725	hypothetical protein	-2.06
GWH15_08685	xerC	-2.09
GWH15_16995	tpiA	-2.10
GWH15_00715	hypothetical protein	-2.26
GWH15_06890	xerC	-2.50
GWH15_00885	hspA	-2.60
GWH15_00780	trpF	-2.80
GWH15_19400	hypothetical protein	-3.05

Table S4: Significantly upregulated proteins in the proteomic profile of *Granulicella* sp. WH15 in high cellobiose concentration. Only statistically significant differentially expressed proteins with a fold change  $\geq 1.0$  are shown.

ORF	Description	log <sub>2</sub> FC
GWH15_02420	Hypothetical protein	4
GWH15_16935	7-carboxy-7-deazaguanine synthase	4
GWH15_15250	ABC transporter ATP-binding protein ytrB	4

ORF (continued)	Description	log <sub>2</sub> FC
GWH15_08630	Al-2 transport protein tqxA	4
GWH15_07165	Aminopeptidase ypdF	4
GWH15_00460	Amylopullulanase	4
GWH15_08480	Anti-sigma-K factor rskA	4
GWH15_08415	Apolipoprotein N-acyltransferase	4
GWH15_00205	Band 7 protein	4
GWH15_05535	Beta-barrel assembly-enhancing protease	4
GWH15_17125	Carbohydrate acetyl esterase/feruloyl esterase	4
GWH15_11910	Carbohydrate transport and metabolism-Glycosyltransferase 36	4
GWH15_15690	Carboxy-terminal processing protease ctpA	4
GWH15_09810	Catabolite control protein A	4
GWH15_18425	CDP-diacylglycerol--glycerol-3-phosphate 3-phosphatidyltransferase	4
GWH15_19395	Cell wall/membrane/envelope biogenesis asmA family	4
GWH15_01995	Cell wall/membrane/envelope biogenesis-asmA family	4
GWH15_09540	Cna B-type protein-transport	4
GWH15_18835	Cobalt-zinc-cadmium resistance protein czcA	4
GWH15_18685	Conserved protein-pfam:duf403	4
GWH15_18690	Conserved protein-pfam:duf403	4
GWH15_09565	Cyclic pyranopterin monophosphate synthase 1	4
GWH15_10075	Cytochrome c oxidase subunit 2	4
GWH15_09055	Cytochrome c-type biogenesis protein ccmF	4
GWH15_10475	Diaminopimelate decarboxylase	4
GWH15_00815	Diguanylate cyclase dosC	4
GWH15_00520	DNA primase	4
GWH15_13725	DNA-directed RNA polymerase subunit omega	4
GWH15_03780	D-ribose-binding periplasmic protein	4
GWH15_02260	Endonuclease mutS2	4
GWH15_00620	Hypothetical protein	4
GWH15_01680	Exopolyphosphatase	4
GWH15_18735	FAD-dependent decaprenylphosphoryl-beta-D-ribofuranose 2-oxidase	4
GWH15_08515	Ferrous iron permease efeU	4
GWH15_00500	Glycogen synthase	4
GWH15_06205	Guanine deaminase	4
GWH15_12695	H(+)/Cl(-) exchange transporter clcA	4
GWH15_00225	Hopanoid biosynthesis associated glycosyl transferase protein hpnI	4
GWH15_19130	HTH-type transcriptional repressor fabR	4
GWH15_12380	Hypothetical protein	4
GWH15_00410	Hypothetical protein	4
GWH15_00175	Hypothetical protein	4
GWH15_01300	Hypothetical protein	4
GWH15_03025	Hypothetical protein	4
GWH15_04195	Hypothetical protein	4
GWH15_04880	Hypothetical protein	4
GWH15_05505	Hypothetical protein	4
GWH15_05985	Hypothetical protein	4
GWH15_06025	Hypothetical protein	4
GWH15_06760	Hypothetical protein	4
GWH15_07215	Hypothetical protein	4
GWH15_08350	Hypothetical protein	4
GWH15_13120	Hypothetical protein	4
GWH15_15045	Hypothetical protein	4
GWH15_15255	Hypothetical protein	4
GWH15_16300	Hypothetical protein	4
GWH15_18130	Hypothetical protein	4
GWH15_02890	Hypothetical protein	4
GWH15_07610	Inorganic ion transport and metabolism-tonB-dependent Receptor	4
GWH15_08030	Inorganic ion transport and metabolism-tonB-dependent Receptor	4
GWH15_15415	Inorganic ion transport and metabolism-tonB-dependent Receptor	4
GWH15_00615	TonB-dependent heme/hemoglobin receptor family protein	4
GWH15_15365	Isoaspartyl dipeptidase	4
GWH15_03790	L-asparaginase 2	4

ORF (continued)	Description	log <sub>2</sub> FC
GWH15_11775	Lexa repressor	4
GWH15_12485	Lipid transport and metabolism-desaturase	4
GWH15_15780	LPS-assembly lipoprotein lptE	4
GWH15_13770	LPS-assembly protein lptD	4
GWH15_15340	Macrolide export ATP-binding/permease protein macB	4
GWH15_15475	Macrolide export ATP-binding/permease protein macB	4
GWH15_03815	Macrolide export protein macA	4
GWH15_12245	Magnesium and cobalt efflux protein corC	4
GWH15_06965	Mannosylfructose-phosphate synthase	4
GWH15_16655	Metallo-beta-lactamase family	4
GWH15_11300	Multidrug resistance protein mdtB	4
GWH15_12080	Multidrug resistance protein mdtB	4
GWH15_19560	Multidrug resistance protein mdtC	4
GWH15_12085	Multidrug resistance protein mdtC	4
GWH15_08245	NADH-quinone oxidoreductase subunit M	4
GWH15_15355	N-formyl-4-amino-5-aminomethyl-2-methylpyrimidine deformylase	4
GWH15_19200	N-formyl-4-amino-5-aminomethyl-2-methylpyrimidine deformylase	4
GWH15_08145	Nuclear protein SET	4
GWH15_15850	Nucleoside permease nupX	4
GWH15_13750	Nucleotide-binding protein	4
GWH15_14450	Outer membrane protein assembly factor bamaA	4
GWH15_03820	Outer membrane protein oprM	4
GWH15_11310	Outer membrane protein oprM	4
GWH15_12090	Outer membrane protein oprM	4
GWH15_16030	Outer membrane protein oprM	4
GWH15_18825	Outer membrane protein oprM	4
GWH15_17110	Penicillin-binding protein 2	4
GWH15_16260	Pfam:DUF811	4
GWH15_14525	PGL/p-HBAD biosynthesis glycosyltransferase	4
GWH15_05440	Phytochrome-like protein cph1	4
GWH15_05490	Poly-beta-1,6-N-acetyl-D-glucosamine synthase	4
GWH15_06970	Polysaccharide export protein	4
GWH15_14210	Polysialic acid transport protein kpsD	4
GWH15_09965	Protein ycel	4
GWH15_15350	Putative ABC transporter ATP-binding protein yknY	4
GWH15_01450	Putative ctpA-like serine protease	4
GWH15_13740	Putative multidrug export ATP-binding/permease protein	4
GWH15_16305	Putative NTE family protein	4
GWH15_17565	Putative thiazole biosynthetic enzyme	4
GWH15_15010	Putative tonB-dependent receptor bfrD	4
GWH15_14825	Putative zinc metalloprotease	4
GWH15_13800	Putative zinc metalloprotease Rip3	4
GWH15_13795	Ribosomal RNA small subunit methyltransferase D	4
GWH15_14980	Ribosomal RNA small subunit methyltransferase H	4
GWH15_16290	RlpA-like protein	4
GWH15_09495	Sensor protein zraS	4
GWH15_01965	Sensory transduction protein lytR	4
GWH15_19165	Signal transduction mechanisms Serine Threonine protein kinase	4
GWH15_09570	Squalene-hopene cyclase	4
GWH15_12830	Thiol-disulfide oxidoreductase resA	4
GWH15_05860	TonB-dependent Receptor	4
GWH15_05950	TonB-dependent Receptor	4
GWH15_12055	TonB-dependent Receptor	4
GWH15_14280	TonB-dependent Receptor	4
GWH15_03535	TonB-dependent receptor plug	4
GWH15_19020	TonB-dependent receptor plug	4
GWH15_09325	Transcriptional activator cadC	4
GWH15_16620	Transcriptional regulatory protein ypdB	4
GWH15_14440	Translocation and assembly module tamB	4
GWH15_13920	Trehalase	4
GWH15_01390	Two component, sigma54 specific, transcriptional regulator, Fis family	4

ORF (continued)	Description	log <sub>2</sub> FC
GWH15_01570	Type II secretion system protein F	4
GWH15_06185	UDP-glucose:undecaprenyl-phosphate glucose-1-phosphate transferase	4
GWH15_11890	Undecaprenyl-phosphate 4-deoxy-4-formamido-L-arabinose transferase	4
GWH15_19395	Hypothetical protein	4
GWH15_03080	Putative mycofactacin radical SAM maturase mftC	2.88
GWH15_17755	TonB-dependent receptor plug	2.68
GWH15_10545	Type II secretion system protein D	2.60
GWH15_17590	Hypothetical protein	2.54
GWH15_10175	Catalase-related peroxidase	2.52
GWH15_07490	Multidrug resistance protein mdtN	2.48
GWH15_07480	Outer membrane efflux protein bepC	2.44
GWH15_05765	TonB-dependent receptor plug	2.42
GWH15_11620	Hypothetical protein	2.32
GWH15_14285	TonB-dependent Receptor	2.28
GWH15_11915	Lipid A export ATP-binding/permease protein msbA	2.13
GWH15_15410	TonB-dependent Receptor	2.12
GWH15_13055	Putative phospholipid ABC transporter-binding protein mlaD	2.12
GWH15_16040	Multidrug resistance protein mdtC	2.11
GWH15_00900	N-formyl-4-amino-5-aminomethyl-2-methylpyrimidine deformylase	2.10
GWH15_01960	Hypothetical protein	2.08
GWH15_13535	Hypothetical protein	2.07
GWH15_01785	TM2 domain	2.02
GWH15_13930	Trehalose synthase/amylase treS	2.02
GWH15_16185	Hypothetical protein	1.99
GWH15_04655	ABC transporter, permease	1.97
GWH15_17630	BON domain	1.96
GWH15_12075	Multidrug resistance protein mdtA	1.95
GWH15_18985	Trehalose-phosphate synthase	1.95
GWH15_05290	Hypothetical protein	1.90
GWH15_15725	ATP-dependent zinc metalloprotease ftsH	1.89
GWH15_13030	Mechanosensitive ion channel	1.89
GWH15_08035	Putative membrane protein mmpL3	1.85
GWH15_00705	Outer membrane protein assembly factor bama	1.83
GWH15_19570	Outer membrane protein toIC	1.83
GWH15_01695	Aminopeptidase N	1.83
GWH15_19225	Sporulation kinase E	1.82
GWH15_13285	Thymidylate kinase	1.81
GWH15_11185	UvrABC system protein A	1.81
GWH15_01225	Toluene efflux pump outer membrane protein ttgF	1.76
GWH15_15395	Peptidase M14, carboxypeptidase A	1.75
GWH15_02935	Multidrug resistance protein mdtB	1.73
GWH15_02030	NADH dehydrogenase-like protein yjID	1.73
GWH15_02940	Multidrug resistance protein mdtA	1.72
GWH15_15995	DNA mismatch repair protein mutL	1.71
GWH15_03075	ABC transporter permease ytrF	1.69
GWH15_15795	Disulphide bond corrector protein dsbC	1.68
GWH15_19215	TonB-dependent receptor plug	1.67
GWH15_05980	TonB-dependent Receptor	1.66
GWH15_06975	Tyrosine-protein kinase ywqD	1.64
GWH15_04000	Tonb-dependent receptor plug	1.63
GWH15_15525	ABC transporter ATP-binding protein natA	1.62
GWH15_14150	Hypothetical protein	1.61
GWH15_01740	Succinyl-diaminopimelate desuccinylase	1.60
GWH15_06990	Hypothetical protein	1.60
GWH15_14235	TonB-dependent Receptor	1.60
GWH15_04050	Hypothetical protein	1.59
GWH15_02945	Decaprenyl-phosphate phosphoribosyltransferase	1.57
GWH15_07680	Catalase-peroxidase	1.54
GWH15_01780	Hypothetical protein	1.54
GWH15_14045	Putative oxidoreductase catD	1.53
GWH15_12475	Pca regulon regulatory protein	1.51

ORF (continued)	Description	log <sub>2</sub> FC
GWH15_02075	Hypothetical protein	1.48
GWH15_01335	Hypothetical protein	1.48
GWH15_12385	Ribosomal protein S12 methyltransferase rimO	1.47
GWH15_00530	Outer membrane protein domain-containing protein	1.47
GWH15_07050	Multidrug export protein emrA	1.45
GWH15_19055	Imidazolonepropionase	1.44
GWH15_12370	Putative efflux system component yknX	1.44
GWH15_09425	Efflux pump membrane transporter bepE	1.44
GWH15_18435	Anthranilate synthase component 1	1.43
GWH15_14490	DNA polymerase/3'-5' exonuclease polX	1.42
GWH15_05965	TonB-dependent Receptor	1.42
GWH15_12430	Putative phospholipid ABC transporter permease protein mlaE	1.41
GWH15_16035	Multidrug resistance protein mdtA	1.41
GWH15_17465	Outer membrane protein assembly factor bamD	1.40
GWH15_02400	TonB family	1.40
GWH15_02910	Hypothetical protein	1.39
GWH15_09000	Putative membrane protein	1.37
GWH15_15800	Thiol-disulfide oxidoreductase resA	1.37
GWH15_12290	Outer membrane lipoprotein Omp16	1.36
GWH15_09420	Outer membrane protein oprM	1.36
GWH15_17035	Glutathione synthase ribosomal protein s6 modification	1.36
GWH15_05770	Prolyl tripeptidyl peptidase	1.35
GWH15_13925	Alpha-1,4-glucan:maltose-1-phosphate maltosyltransferase 1	1.34
GWH15_02605	Methionine aminopeptidase 1	1.33
GWH15_08560	4,4'-diaponeurosporenoate glycosyltransferase	1.30
GWH15_11595	Putative mscs family protein ykuT	1.30
GWH15_07225	Hypothetical protein	1.29
GWH15_13275	Hypothetical protein	1.28
GWH15_07045	Outer membrane protein oprM	1.28
GWH15_11845	Vitamin B12 transporter btuB	1.27
GWH15_19245	Biopolymer transport protein exbD	1.26
GWH15_01440	Glycosyl transferase family	1.23
GWH15_12815	TonB-dependent receptor plug	1.23
GWH15_06900	BON domain	1.22
GWH15_03995	Feruloyl esterase	1.22
GWH15_12700	TonB family	1.22
GWH15_18875	TonB-dependent receptor plug	1.21
GWH15_13410	HTH-type transcriptional regulator lutR	1.19
GWH15_09020	Hypothetical protein	1.19
GWH15_04110	2-dehydro-3-deoxy-D-gluconate 5-dehydrogenase	1.18
GWH15_02670	Translation initiation factor IF-2	1.18
GWH15_18510	Biodegradative arginine decarboxylase	1.17
GWH15_05295	Dispase autolysis-inducing protein	1.15
GWH15_19675	Membrane protein insertase yidC	1.15
GWH15_07605	Response regulator protein vraR	1.15
GWH15_00730	30S ribosomal protein S1	1.14
GWH15_02465	30S ribosomal protein S12	1.13
GWH15_12305	Hypothetical protein	1.13
GWH15_19615	DNA-binding protein HU	1.12
GWH15_17135	Rod shape-determining protein mreB	1.11
GWH15_03785	L-asparaginase 2	1.11
GWH15_15505	Energy-dependent translational throttle protein ettA	1.09
GWH15_18520	Exodeoxyribonuclease 7 large subunit	1.08
GWH15_16085	Hypothetical protein	1.07
GWH15_14870	tRNA threonylcarbamoyladenosine biosynthesis protein tsaE	1.07
GWH15_03680	Vitamin B12-dependent ribonucleoside-diphosphate reductase	1.06
GWH15_05990	Hypothetical protein	1.06
GWH15_12285	Protein tolB	1.05
GWH15_11850	Hypothetical protein	1.05
GWH15_01330	Putative nicotinate-nucleotide pyrophosphorylase [carboxylating]	1.04
GWH15_11780	Hypothetical protein	1.03

ORF (continued)	Description	log <sub>2</sub> FC
GWH15_19025	Quinate/shikimate dehydrogenase (quinone)	1.03
GWH15_04580	Methionine synthase	1.02
GWH15_07455	Protein translocase subunit secA	1.01

Table S5: Significantly downregulated proteins in the proteomic profile of *Granulicella* sp. WH15 in high cellobiose concentration. Only statistically significant differentially expressed proteins with a fold change  $\leq -1.0$  are shown.

ORF	Description	log <sub>2</sub> FC
GWH15_02345	3-isopropylmalate dehydratase small subunit 1	-4.00
GWH15_14090	Formate dehydrogenase	-4.00
GWH15_00995	Glutamate synthase [NADPH] small chain	-4.00
GWH15_00610	Glycerate dehydrogenase	-4.00
GWH15_17605	Homoserine O-acetyltransferase	-4.00
GWH15_06475	1-deoxy-D-xylulose-5-phosphate synthase	-4.00
GWH15_06375	4-hydroxythreonine-4-phosphate dehydrogenase 2	-4.00
GWH15_01205	Dephospho-coA kinase	-4.00
GWH15_08325	L-2,4-diaminobutyrate decarboxylase	-4.00
GWH15_10235	Multifunctional cyclase-dehydratase-3-O-methyl transferase tcmN	-4.00
GWH15_11220	Phosphomethylpyrimidine synthase	-4.00
GWH15_18315	Phosphopantetheine adenyltransferase	-4.00
GWH15_07695	Pyrroloquinoline-quinone synthase	-4.00
GWH15_02155	Riboflavin biosynthesis protein ribD	-4.00
GWH15_18275	3-deoxy-manno-octulosonate cytidyltransferase	-4.00
	Acyl-[acyl-carrier-protein]-UDP-N-acetylglucosamine	
GWH15_01640	O-Acyltransferase	-4.00
GWH15_15135	Lipopolysaccharide heptosyltransferase 1	-4.00
GWH15_15130	Tetraacyldisaccharide 4'-kinase	-4.00
GWH15_08130	UDP-3-O-acylglucosamine N-acyltransferase	-4.00
GWH15_12280	UDP-N-acetylenolpyruvoylglucosamine reductase	-4.00
GWH15_06130	Acetyl-coA:oxalate coA-transferase	-4.00
GWH15_07765	Phenylacetaldehyde dehydrogenase	-4.00
GWH15_11565	Biphenyl dioxygenase system ferredoxin subunit	-4.00
GWH15_11410	N-acetylglucosamine-6-phosphate deacetylase	-4.00
GWH15_07550	1,5-anhydro-D-fructose reductase	-4.00
GWH15_13480	2-dehydro-3-deoxy-D-gluconate 5-dehydrogenase	-4.00
GWH15_07735	2-hydroxy-3-oxopropionate reductase	-4.00
GWH15_17540	2-methylcitrate dehydratase	-4.00
GWH15_17545	2-methylcitrate synthase	-4.00
GWH15_05100	5'-nucleotidase	-4.00
GWH15_07745	Beta-galactosidase bgaB	-4.00
GWH15_13400	Beta-xylosidase	-4.00
GWH15_07310	Inosose dehydratase	-4.00
GWH15_10460	NADH-quinone oxidoreductase subunit I	-4.00
GWH15_09940	Pyrethroid hydrolase	-4.00
GWH15_06155	Ribulose biphosphate carboxylase-like protein 2	-4.00
GWH15_08005	Sorbitol dehydrogenase	-4.00
GWH15_06480	Transketolase 2	-4.00
GWH15_18410	D-xylulose 1-dehydrogenase	-4.00
GWH15_03275	Release factor glutamine methyltransferase	-4.00
GWH15_08570	6-carboxy-5,6,7,8-tetrahydropterin synthase	-4.00
GWH15_06145	Hypothetical protein	-4.00
GWH15_16100	Hypothetical protein	-4.00
GWH15_01830	Transcriptional regulatory protein yycF	-4.00
GWH15_13365	2-keto-3-deoxy-L-fuconate dehydrogenase	-4.00
GWH15_11615	3',5'-cyclic adenosine monophosphate phosphodiesterase cpdA	-4.00
GWH15_11945	4-hydroxy-4-methyl-2-oxoglutarate aldolase	-4.00
GWH15_17960	4-hydroxy-4-methyl-2-oxoglutarate aldolase	-4.00
GWH15_19220	6'''-hydroxyparomomycin C oxidase	-4.00

ORF (continued)	Description	log2 FC
GWH15_05265	Acetylxylylase	-4.00
GWH15_15430	Acyl-coA dehydrogenase	-4.00
GWH15_16250	Acyl-coA dehydrogenase	-4.00
GWH15_03975	Acyl-coenzyme A thioesterase paal	-4.00
GWH15_17610	Beta-barrel assembly-enhancing protease	-4.00
GWH15_12730	Cellulose synthase operon protein C	-4.00
GWH15_06620	D-galactonate dehydratase	-4.00
GWH15_17965	D-galactonate dehydratase	-4.00
GWH15_11940	D-galactonate dehydratase family member	-4.00
GWH15_02130	Endonuclease 4	-4.00
GWH15_00665	Endo-polygalacturonase	-4.00
GWH15_17915	Exo-poly-alpha-D-galacturonosidase	-4.00
GWH15_09450	Glutamate-pyruvate aminotransferase alaA	-4.00
GWH15_02870	Hydroxymethylglutaryl-coa lyase yngG	-4.00
GWH15_08530	Hydroxypyruvate isomerase	-4.00
GWH15_00145	Hypothetical protein	-4.00
GWH15_00585	Hypothetical protein	-4.00
GWH15_02685	Hypothetical protein	-4.00
GWH15_03305	Hypothetical protein	-4.00
GWH15_03765	Hypothetical protein	-4.00
GWH15_03835	Hypothetical protein	-4.00
GWH15_03840	Hypothetical protein	-4.00
GWH15_05465	Hypothetical protein	-4.00
GWH15_06125	Hypothetical protein	-4.00
GWH15_06295	Hypothetical protein	-4.00
GWH15_06310	Hypothetical protein	-4.00
GWH15_06330	Hypothetical protein	-4.00
GWH15_06345	Hypothetical protein	-4.00
GWH15_06600	Hypothetical protein	-4.00
GWH15_07205	Hypothetical protein	-4.00
GWH15_07540	Hypothetical protein	-4.00
GWH15_07555	Hypothetical protein	-4.00
GWH15_07565	Hypothetical protein	-4.00
GWH15_07740	Hypothetical protein	-4.00
GWH15_07750	Hypothetical protein	-4.00
GWH15_07795	Hypothetical protein	-4.00
GWH15_07975	Hypothetical protein	-4.00
GWH15_08075	Hypothetical protein	-4.00
GWH15_08600	Hypothetical protein	-4.00
GWH15_08945	Hypothetical protein	-4.00
GWH15_09720	Hypothetical protein	-4.00
GWH15_10775	Hypothetical protein	-4.00
GWH15_12310	Hypothetical protein	-4.00
GWH15_12655	Hypothetical protein	-4.00
GWH15_12725	Hypothetical protein	-4.00
GWH15_13405	Hypothetical protein	-4.00
GWH15_13455	Hypothetical protein	-4.00
GWH15_13460	Hypothetical protein	-4.00
GWH15_15770	Hypothetical protein	-4.00
GWH15_16360	Hypothetical protein	-4.00
GWH15_16925	Hypothetical protein	-4.00
GWH15_17970	Hypothetical protein	-4.00
GWH15_18790	Hypothetical protein	-4.00
GWH15_19005	Hypothetical protein	-4.00
GWH15_11130	Hypothetical protein	-4.00
GWH15_09830	Hypothetical protein	-4.00
GWH15_06095	Hypothetical protein	-4.00
GWH15_17550	Methylisocitrate lyase	-4.00
GWH15_05095	Methylxanthine N1-demethylase ndmA	-4.00
GWH15_00990	NAD-dependent dihydropyrimidine dehydrogenase subunit preA	-4.00
GWH15_13220	Phosphoribosyl-AMP cyclohydrolase	-4.00

ORF (continued)	Description	log2 FC
GWH15_00845	Prephenate dehydrogenase	-4.00
GWH15_18405	Putative 3-hydroxybutyryl-coa dehydrogenase	-4.00
GWH15_02095	Putative formate dehydrogenase	-4.00
GWH15_12060	Putative N-succinyl-diaminopimelate aminotransferase dapC	-4.00
GWH15_12955	Putative prophage major tail sheath protein	-4.00
GWH15_17805	Putative succinyl-coA:3-ketoacid coenzyme A transferase subunit B	-4.00
GWH15_03720	Reducing end xylose-releasing exo-oligoxylanase	-4.00
GWH15_09815	Retaining alpha-galactosidase	-4.00
GWH15_15040	Short-chain-enoyle-coa hydratase	-4.00
GWH15_13515	UDP-glucose 4-epimerase	-4.00
GWH15_07980	Hypothetical protein	-3.77
GWH15_07970	Hypothetical protein	-3.36
GWH15_07865	Putative acyl-coA dehydrogenase	-3.12
GWH15_07780	Gluconolactonase	-2.85
GWH15_07855	Putative 3-hydroxyacyl-coa dehydrogenase	-2.66
GWH15_13495	Virginiamycin B lyase	-2.42
GWH15_17530	Hypothetical protein	-2.40
GWH15_06300	Beta-galactosidase bgaA	-2.40
GWH15_07860	3-ketoacyl-coA thiolase	-2.28
GWH15_06320	Hypothetical protein	-2.16
GWH15_01715	Electron transfer flavoprotein subunit beta	-2.13
GWH15_18430	Glutamate dehydrogenase	-2.01
GWH15_07990	Extracellular exo-alpha-L-arabinofuranosidase	-1.97
GWH15_08000	Gluconate 5-dehydrogenase	-1.96
GWH15_06150	Non-reducing end beta-L-arabinofuranosidase	-1.91
GWH15_17820	Hypothetical protein	-1.77
GWH15_08445	Hypothetical protein	-1.73
GWH15_01710	Electron transfer flavoprotein subunit alpha	-1.71
GWH15_18330	Hypothetical protein	-1.71
GWH15_13235	Histidinol-phosphate aminotransferase 2	-1.70
GWH15_13420	Protein tolB	-1.70
GWH15_07965	Serine/threonine-protein kinase pknD	-1.69
GWH15_14310	Dihydroxy-acid dehydratase	-1.61
GWH15_07530	Hypothetical protein	-1.60
GWH15_03715	Hypothetical protein	-1.60
GWH15_11790	Metallo-beta-lactamase L1	-1.59
GWH15_09775	NAD-dependent malic enzyme	-1.58
GWH15_00385	Putative oxidoreductase ydBc	-1.54
GWH15_02245	1,4-beta-D-glucan glucohydrolase	-1.52
GWH15_11350	Putative KHG/KDPG aldolase	-1.51
GWH15_17080	Hypothetical protein	-1.49
GWH15_13390	L-rhamnonate dehydratase	-1.49
GWH15_01535	6-phosphogluconate dehydrogenase, NADP(+)-dependent	-1.49
GWH15_05340	General stress protein 69	-1.46
GWH15_13415	Xylitol oxidase	-1.46
GWH15_17570	D-galactarolactone cycloisomerase	-1.45
GWH15_07145	Long-chain-fatty-acid--coa ligase fadd15	-1.43
GWH15_16015	Putative propionyl-coa carboxylase beta chain 5	-1.42
GWH15_02240	Capsular glucan synthase	-1.42
GWH15_08525	Inosose dehydratase	-1.40
GWH15_01075	Catechol-2,3-dioxygenase	-1.36
GWH15_17815	Aldose 1-epimerase	-1.35
GWH15_14330	Scyllo-inositol 2-dehydrogenase (NAD(+))	-1.34
GWH15_18470	Adenine phosphoribosyltransferase	-1.32
GWH15_07615	4-hydroxy-4-methyl-2-oxoglutarate aldolase	-1.30
GWH15_02610	Monoterpene epsilon-lactone hydrolase	-1.26
GWH15_04030	Cystathionine beta-lyase metC	-1.23
GWH15_05255	Phosphoheptose isomerase	-1.23
GWH15_06910	4-alpha-glucanotransferase	-1.23
GWH15_11420	Copper-exporting P-type atpase A	-1.21
GWH15_13265	Hypothetical protein	-1.21

ORF (continued)	Description	log2 FC
GWH15_14105	Free methionine-R-sulfoxide reductase	-1.20
GWH15_13500	Methylmalonate semialdehyde dehydrogenase [acylating]	-1.19
GWH15_11370	Gluconate 5-dehydrogenase	-1.17
GWH15_09530	Riboflavin biosynthesis protein ribbA	-1.17
GWH15_18555	Ribonuclease R	-1.16
GWH15_06590	Hypothetical protein	-1.16
GWH15_14315	Hypothetical protein	-1.16
GWH15_12790	2-hydroxyhexa-2,4-dienoate hydratase	-1.14
GWH15_00640	Hypothetical protein	-1.14
GWH15_10795	Xylan 1,4-beta-xylosidase	-1.13
GWH15_02440	Acetyl-coenzyme A synthetase	-1.13
GWH15_11970	Aldehyde reductase yahK	-1.12
GWH15_06545	Putative glycerophosphoryl diester phosphodiesterase 1	-1.11
GWH15_02965	Hypothetical protein	-1.11
GWH15_13360	Ureidoglycolate lyase	-1.11
GWH15_14415	P-protein	-1.10
GWH15_11385	Hypothetical protein	-1.10
GWH15_05145	Hypothetical protein	-1.08
GWH15_15710	Putative glucose-6-phosphate 1-epimerase	-1.07
GWH15_06770	Hypothetical protein	-1.06
GWH15_14470	Hypothetical protein	-1.06
GWH15_14895	Oxalate decarboxylase oxdC	-1.03
GWH15_17295	Hypothetical protein	-1.03
GWH15_14850	Farnesyl diphosphate synthase	-1.03
GWH15_17980	Pyruvate dehydrogenase [ubiquinone]	-1.02
GWH15_08905	UDP-glucose 4-epimerase	-1.01
GWH15_10410	Trigger factor	-1.00

Table S6: Number of significantly up and downregulated proteins assigned to KEGG metabolic pathways in the proteomic profile of *Granulicella* strain WH15 in high cellobiose conditions.

KEGG metabolic pathways	Upregulated	Downregulated
Metabolic pathways	15	56
Biosynthesis of secondary metabolites	6	22
Biosynthesis of antibiotics	3	19
Microbial metabolism in diverse environments	1	14
Carbon metabolism	1	12
Biosynthesis of amino acids	3	11
Fatty acid metabolism	1	8
Lipopolysaccharide biosynthesis	0	6
Fatty acid biosynthesis	0	5
Butanoate metabolism	0	5
Propanoate metabolism	0	5
Valine, leucine and isoleucine degradation	0	5
Starch and sucrose metabolism	2	4
Galactose metabolism	0	4
Amino sugar and nucleotide sugar metabolism	0	4
Glyoxylate and dicarboxylate metabolism	1	4
Fatty acid degradation	0	4
Phenylalanine, tyrosine and tryptophan biosynthesis	1	4
Pantothenate and CoA biosynthesis	0	4
Benzoate degradation	0	4
Pentose phosphate pathway	0	4
Other glycan degradation	0	3
Quorum sensing	3	3
Novobiocin biosynthesis	0	3
Phenylalanine metabolism	1	3
Cysteine and methionine metabolism	1	3
Methane metabolism	0	3
2-Oxocarboxylic acid metabolism	0	3

KEGG metabolic pathways (continued)	Upregulated	Downregulated
Cyanoamino acid metabolism	0	2
Folate biosynthesis	0	2
Glycolysis / Gluconeogenesis	0	2
Tyrosine metabolism	0	2
Fructose and mannose metabolism	0	2
Histidine metabolism	0	2
Pentose and glucuronate interconversions	0	2
Pyruvate metabolism	0	2
Nitrogen metabolism	0	2
Arginine biosynthesis	0	2
Synthesis and degradation of ketone bodies	0	2
Valine, leucine and isoleucine biosynthesis	0	2
beta-Alanine metabolism	0	2
Riboflavin metabolism	0	2
Geraniol degradation	0	2
Alanine, aspartate and glutamate metabolism	0	2
Biotin metabolism	0	1
ABC transporters	4	1
Sulfur metabolism	0	1
Bacterial chemotaxis	2	1
Arginine and proline metabolism	1	1
Thiamine metabolism	0	1
Glycine, serine and threonine metabolism	0	1
Xylene degradation	0	1
Purine metabolism	2	1
Glutathione metabolism	2	1
Oxidative phosphorylation	3	1
Cationic antimicrobial peptide (CAMP) resistance	1	1
Degradation of aromatic compounds	0	1
Two-component system	9	1
C5-Branched dibasic acid metabolism	0	1
Pyrimidine metabolism	1	1
RNA degradation	0	1
Terpenoid backbone biosynthesis	0	1
alpha-Linolenic acid metabolism	0	1
Sphingolipid metabolism	1	1
Selenocompound metabolism	1	1
Glycerophospholipid metabolism	1	1
D-Glutamine and D-glutamate metabolism	0	1
Peptidoglycan biosynthesis	0	1
Chlorocyclohexane and chlorobenzene degradation	0	1
Inositol phosphate metabolism	0	1
Biosynthesis of unsaturated fatty acids	1	0
Lysine biosynthesis	1	0
Sesquiterpenoid and triterpenoid biosynthesis	1	0
beta-Lactam resistance	2	0
Bacterial secretion system	4	0
Tryptophan metabolism	2	0
Ribosome	2	0
Protein export	2	0
Nucleotide excision and repair	1	0
Mismatch repair	2	0
One carbon pool by folate	1	0
DNA replication	1	0
RNA polymerase	1	0
Nicotinate and nicotinamide metabolism	1	0
Phenazine biosynthesis	1	0

